

Multi-genome comparisons reveal gain-and-loss evolution of the *anti-Mullerian hormone receptor type 2* gene, an old master sex determining gene, in Percidae

Running title: Genomic evolution of sex determination in Percidae

Heiner Kuhl^{1*}, Peter T Euclide², Christophe Klopp³, Cedric Cabau⁴, Margot Zahm³, Céline Roques⁵, Carole Iampietro⁵, Claire Kuchly⁵, Cécile Donnadieu⁵, Romain Feron^{6,7}, Hugues Parrinello⁸, Charles Poncet⁹, Lydia Jaffrelo⁹, Carole Confolent⁹, Ming Wen^{10,11}, Amaury Herpin¹⁰, Elodie Jouanno¹⁰, Anastasia Bestin¹², Pierrick Haffray¹², Romain Morvezen¹², Taina Rocha de Almeida¹³, Thomas Lecocq¹³, Bérénice Schaerlinger¹³, Dominique Chardard¹³, Daniel Źarski¹⁴, Wes Larson¹⁵, John H. Postlethwait¹⁶, Serik Timirkhanov¹⁷, Werner Kloas¹, Sven Wuertz¹, Matthias Stöck¹, Yann Guiguen^{10*}

Affiliations

¹ Leibniz-Institute of Freshwater Ecology and Inland Fisheries – IGB (Forschungsverbund Berlin), Müggelseedamm 301/310, D-12587 Berlin, Germany.

² Department of Forestry and Natural Resources | Illinois-Indiana Sea Grant, Purdue University, West Lafayette, Indiana, USA

³ Sigenae, Plateforme Bioinformatique, Genotoul, BioinfoMics, UR875 Biométrie et Intelligence Artificielle, INRAE, Castanet-Tolosan, France

⁴ Sigenae, GenPhySE, Université de Toulouse, INRAE, ENVT, Castanet Tolosan, France

⁵ INRAE, US 1426, GeT-PlaGe, Genotoul, Castanet-Tolosan, France

⁶ Department of Ecology and Evolution, University of Lausanne, Lausanne, Switzerland.

⁷ Swiss Institute of Bioinformatics, Lausanne, Switzerland.

⁸ Montpellier GenomiX (MGX), c/o Institut de Génomique Fonctionnelle, 141 rue de la Cardonille, 34094, Montpellier Cedex 05, France

⁹ GDEC Gentyane, INRAE, Université Clermont Auvergne, Clermont-Ferrand, France

¹⁰ INRAE, LPGP, 35000, Rennes, France.

¹¹ State Key Laboratory of Developmental Biology of Freshwater Fish, College of Life Science, Hunan Normal University, Changsha, China

¹² SYSAF, Station INRAE-LPGP, Campus de Beaulieu, 35042, Rennes cedex, France

¹³ University of Lorraine, INRAE, UR AFPA, Nancy, France

¹⁴ Department of Gamete and Embryo Biology, Institute of Animal Reproduction and Food Research, Polish Academy of Sciences, ul. Tuwima 10, 10-748, Olsztyn, Poland

¹⁵ National Oceanographic and Atmospheric Administration, National Marine Fisheries Service, Alaska Fisheries Science Center, Auke Bay Laboratories, 17109 Point Lena Loop Road, Juneau, AK, 99801, USA

¹⁶ Institute of Neuroscience, University of Oregon, Eugene, OR, 97403, USA.

¹⁷ Sea Biology LLP, Almaty, Kazakhstan.

* corresponding authors:

Heiner Kuhl (Heiner.Kuhl@igb-berlin.de) and Yann Guiguen (yann.guiguen@inrae.fr)

ABSTRACT

The Percidae family comprises many fish species of major importance for aquaculture and fisheries. Based on three new chromosome-scale assemblies in *Perca fluviatilis*, *Perca schrenkii* and *Sander vitreus* along with additional percid fish reference genomes, we provide an evolutionary and comparative genomic analysis of their sex-determination systems. We explored the fate of a duplicated anti-Mullerian hormone receptor type-2 gene (*amhr2bY*), previously suggested to be the master sex determining (MSD) gene in *P. flavescens*. Phylogenetically related and structurally similar *amhr2* duplications (*amhr2b*) were found in *P. schrenkii* and *Sander lucioperca*, potentially dating this duplication event to their last common ancestor around 19-27 Mya. In *P. fluviatilis* and *S. vitreus*, this *amhr2b* duplicate has been lost while it was subject to amplification in *S. lucioperca*. Analyses of the *amhr2b* locus in *P. schrenkii* suggest that this duplication could be also male-specific as it is in *P. flavescens*. In *P. fluviatilis*, a relatively small (100 kb) non-recombinant sex-determining region (SDR) was characterized on chromosome-18 using population-genomics approaches. This SDR is characterized by many male-specific single-nucleotide variants (SNVs) and no large duplication/insertion event, suggesting that *P. fluviatilis* has a male heterogametic sex determination system (XX/XY), generated by allelic diversification. This SDR contains six annotated genes, including three (*c18h1orf198*, *hmdl1*, *tbc1d32*) with higher expression in testis than ovary. Together, our results provide a new example of the highly dynamic sex chromosome turnover in teleosts and provide new genomic resources for Percidae, including sex-genotyping tools for all three known *Perca* species.

Keywords: sex-determination, genome, perches, pikeperches, sex-chromosomes

INTRODUCTION

The percid family (Percidae, Rafinesque) encompasses a large number (over 250) of diverse ecologically and economically important fish species, assigned to 11 genera [1]. Two genera, *Perca* and *Sander* are found across both Eurasia and North America, with separate species native to each continent (Eurasia: *Perca fluviatilis* / *Sander lucioperca*; North America: *Perca flavescens* / *Sander vitreus*). Percids are classically described as typical freshwater species of the Northern hemisphere, even if some species can be regularly found in brackish waters (e.g. *Sander lucioperca*, *Perca fluviatilis*). In the context of declining fisheries over the past few decades, but also due to their high value and good market acceptance, four percid species - *Perca flavescens* (yellow perch) and *Sander vitreus* (walleye) in North America and *P. fluviatilis* (European perch) and *S. lucioperca* (zander) in Eurasia are particularly promising for aquaculture. Rearing these fish in recirculation aquaculture systems (RAS) allows for a control of reproduction and a year-round production of stocking fish [2,3]. Although year-round production represents an important competitive goal, current production targets premium markets and an up-scaling of production faces several bottlenecks [4].

Among these bottlenecks is better control of the sex of developing individuals because in both *Perca* and *Sander* genera, females grow faster than males [5,6]. Due to faster female growth (up to 25-50% in *Perca*, 10% in *Sander*), all-female stocks are highly desirable. In *Perca fluviatilis*, sex determination has been assumed to be male heterogametic (XX/XY) based on gynogenesis or hormonal treatment experiments [7,8]. These methodologies also produced genetic female but phenotypic male individuals (neomales) that can be used to produce all-female stocks by crossing normal XX females with these chromosomally XX neomales. This approach would, however, greatly benefit from a reliable sexing method allowing the identification of genetic sex early during development to select rare genetically XX neomales as future breeders in aquaculture. In *P. flavescens*, an XX female/XY male heterogametic genetic sex determination system has been also recently uncovered, with duplication / insertion of an anti-Mullerian hormone receptor type 2 (*amhr2*) gene as a potential master sex determining gene [9].

Genes encoding many members of the transforming growth factor beta (TGF- β) gene family, including anti-Mullerian hormone (*amh*) and anti-Mullerian hormone receptor type-2 (*amhr2*), have repeatedly and independently evolved as master sex-determining (MSD) genes in vertebrates [10]. For instance, *amh* has been characterized or suspected to be the MSD gene in pikes [11,12], Nile tilapia [13], lumpfish [14], *Sebastes* rockfish [15], lingcod [16], and Patagonian pejerrey [17]. The cognate receptor gene of Amh, *amhr2*, has also been found as a potential MSD gene in Pangasiidae [18], Takifugu [19], Ayu [20], common seadragon and alligator pipefish [21], as well as in yellow perch [9]. The repeated and independent recruitment of TGF- β receptors, including *Amhr2*, in teleost fish sex determination is even more puzzling as many of these MSD genes, encoding a TGF β receptor, share a similar N-terminal

truncation [9,18,21], supporting their evolution towards a ligand-independent mechanism of action [18]. Therefore, the extent of evolutionary conservation of the Y-linked *amhr2bY* gene found in yellow perch in closely related species (genus *Perca* and *Sander*) is an important question with implications for better sex-control in these aquaculture species and for understanding the evolution of sex linkage and protein structure.

Regarding genomics of Percidae, two long-read reference quality genome assemblies have recently been published for *P. flavescens* and *S. lucioperca* [9,22]. While for *P. fluviatilis* and *S. vitreus* only draft genomes, generated from short-read sequencing, have been available [23]. Here, we provide three new long-read chromosome-scale genome assemblies for *P. fluviatilis*, *P. schrenkii* and *Sander vitreus* and thus complete genomic resources for the economically most important species of Percidae. These data enabled us to develop PCR-assays for sexing of all three *Perca* species and shed light on gene gain-and-loss in the evolution of an old MSD gene in Percidae.

MATERIAL AND METHODS

Biological samples

In *Perca fluviatilis*, high molecular weight (HMW) genomic DNA (gDNA) for genome sequencing was extracted from a blood sample of a male called “Pf_M1” (BioSample ID SAMN12071746) from the aquaculture facility of the University de Lorraine, Nancy, France. Blood (0.5 ml) was sampled and directly stored in 25 ml of a TNES-Urea lysis buffer (TNES-Urea: 4 M urea; 10 mM Tris-HCl, pH 7.5; 125 mM NaCl; 10 mM EDTA; 1% SDS). HMW gDNA was extracted from the TNES-urea buffer using a slightly modified phenol/chloroform protocol as described [12]. For the chromosome contact map (Hi-C), 1.5 ml of blood was taken from the same animal and slowly (1 K/min) cryopreserved with 15 % dimethyl sulfoxide (DMSO) in a Mr. Frosty Freezing Container (ThermoFisher) at -80°C. Additional fin clip samples for RAD-Sequencing (RAD-Seq), Pool-Sequencing (Pool-Seq) or sex-genotyping assays were collected and stored in 90% ethanol, either at the Lucas Perche aquaculture facility (Le Moulin de Cany, 57170 Hampont, France), at Kortowskie Lake in Poland, or at Mueggelsee Lake in Germany.

Samples of *Perca schrenkii* were obtained for genome sequencing and sex genotyping from male and female wild catches at lake Alakol, Kazakhstan (46.328 N, 81.374 E). Different organs and tissues (brain, liver, muscle, ovary, testis) were sampled for genome and transcriptome sequencing (Biosample ID SAMN15143703) and stored in RNAlater. HMW gDNA for genome sequencing was extracted from brain tissue of the male *P. schrenkii* individual, using the MagAttract HMW DNA Kit (Qiagen, Germany).

Total RNA for transcriptome sequencing was isolated using a standard Trizol protocol, in combination with the RNAeasy Mini Kit (Qiagen, Germany).

For genome sequencing of *Sander vitreus* a fin clip of a male was sampled by Ohio Department of Natural Resources (Ohio, DNR) in spring 2017 and stored in 96% ethanol. The *S. vitreus* sample called “19-12246” originated from Maumee River, Ohio [41.554 N; -83.6605W]. DNA was extracted using the DNeasy Tissue Kit (Qiagen). Short DNA fragments were removed/reduced by size-selective, magnetic-bead purification using 0.35x of sample volume AMPure beads (Beckmann-Coulter) and two washing steps with 70% ethanol.

Sequencing

Genomic sequencing of *P. fluviatilis* was carried out using a combination of 2x250 bp Illumina short-reads, Oxford Nanopore long reads and a chromosome contact map (Hi-C). For long-read sequencing, DNA was sheared to 20 kb using the megaruptor system (Diagenode). ONT (Oxford nanopore technologies) library preparation and sequencing was performed using 5 µg of sheared DNA and ligation sequencing kits SQK-LSK108 or SQK-LSK109, according to the manufacturer's instructions. The libraries were loaded at a concentration of 0.005 to 0.1 pmol and sequenced for 48 h on 11 GridION R9.4 or R9.4.1 flowcells. Short read wgs (whole genome shotgun) sequencing for consensus polishing of noisy long read assemblies was carried out by shearing the HMW DNA to approximately 500 bp fragments and using the Illumina Truseq X kit, according to the manufacturer's instructions. The library was sequenced using a read length of 250 bp in paired-end mode (HiSeq 3000, Illumina, California, USA). Hi-C library generation for chromosome assembly was carried out according to a protocol adapted from Rao *et al.* 2014 [24]. The blood sample was spun down, and the cell pellet was resuspended and fixed in 1% formaldehyde. Five million cells were processed for the Hi-C library. After overnight-digestion with *HindIII* (NEB), DNA-ends were labeled with Biotin-14-DCTP (Invitrogen), using Klenow fragment (NEB) and re-ligated. A total of 1.4 µg of DNA was sheared to an average size of 550 bp (Covaris). Biotinylated DNA-fragments were pulled down using M280 Streptavidin Dynabeads (Invitrogen) and ligated to PE adaptors (Illumina). The Hi-C library was amplified using PE primers (Illumina) with 10 PCR amplification cycles. The library was sequenced using a HiSeq3000 (Illumina, California, USA), generating 150 bp paired-end reads.

Genomic sequencing of *P. schrenkii* and *S. vitreus* was carried out using Oxford Nanopore long reads on a MinION nanopore sequencer (Oxford Nanopore Technologies, UK) in combination with the MinIT system. Several libraries were constructed using the tagmentation-based SQK-RAD004 kit with varying amounts of input DNA (0.4 to 1.2 µg) from a male individual or using the ligation approach of the SQK-LSK109 kit (input DNA 2 µg). Libraries were sequenced on R9.4.1 flowcells with variable run times and

exonuclease washes by the EXP-WSH003 kit to remove pore blocks and improve the data yield. Short-read wgs-sequencing of *P. schrenkii* was conducted at BGI (BGI Genomics Co., Ltd.). A *P. schrenkii* male and a female wgs library (300 bp fragment length) were constructed and paired end reads of 150 bp length were generated on an Illumina Hiseq4000 system. Public short-read wgs data of *S. vitreus* were obtained from the NCBI Sequence Read Archive (SRA) using the accession SRR9711286. Transcriptome sequencing of six *P. schrenkii* samples (female brain, male brain, male muscle, female liver, ovary and testis) was conducted at BGI. Transcriptome-sequencing libraries were constructed from total RNA, applying enrichment of mRNA with oligo(dT) hybridization, mRNA fragmentation, random hexamer cDNA synthesis, size selection and PCR amplification. Sequencing of 150 bp paired-end reads was performed by an Illumina HiSeq X Ten system.

Genome assembly of Perca fluviatilis

Residual adaptor sequences in ONT GridION long reads were trimmed and split by Porechop (v0.2.1) [25]. Reads longer than 9999 bp were assembled by SmartDeNovo (May-2017) [26] using default parameters. Long reads were remapped to the SmartDeNovo contigs by Minimap2 (v2.7) [27] and Racon (v1.3.12) [28] was used to polish the consensus sequence. In a second round of polishing, Illumina short-reads were mapped by BWA mem (v0.7.12-r1039) [29] to the contigs, which were subsequently polished by Pilon (v1.223) [30]. The chromosome-scale assembly was performed by mapping Hi-C data to the assembled contigs, using the Juicer pipeline (v1.5.6) [31] and subsequent scaffolding by 3D-DNA (v180114) [32]. Juicebox (v1.8.8) [33] was used to manually review and curate the chromosome-level scaffolds. A final gap-closing step, applying long reads and LR_gapcloser (v1.1, default parameters) [34], further increased contig length. After gap-closing, a final consensus sequence polishing step was performed by mapping short reads to the scaffolds, sequence variants (1/1 genotypes were considered as corrected errors) were detected with Freebayes (v0.9.7) [35] and written to a vcf-file. The final fasta file was then generated by vcf-consensus from Vcftools (v0.1.15, default parameters).

Genome assembly of Perca schrenkii and Sander vitreus

Illumina short reads were trimmed using Trimmomatic (v0.35) [36]. Short reads were assembled using a custom compiled high kmer version of idba-ud (v1.1.1) [37] with kmer size up to 252. The resulting contigs were mapped against available Percidae genomes (*P. flavescens*, *P. fluviatilis* and *S. lucioperca*) by Minimap2 and analysis of overall mapped sequence length resulted in *P. schrenkii* aligned best with *P. flavescens* and *S. vitreus* aligned best with *S. lucioperca*. According to the benchmarks published in [38], the publicly available chromosome-level assembly of *P. flavescens* (RefSeq: GCF_004354835.1)

could be used to aid the chromosome assembly of *P. schrenkii* as follows: ONT MinION long reads (male sample) were trimmed and split using Porechop (v0.2.1) [25]. The inhouse developed CSA method (v2.6) [38], was used to assemble the *P. schrenkii* genome from long-read data and short-read contigs and to infer chromosomal scaffolds using the *P. flavescens* reference genome. CSA parameters were optimized to account for relatively low long-read sequencing coverage and hybrid assembly of long reads and short-read contigs:

```
CSA2.6.pl -r longreads.fa.gz -g P.flavescens.fa -k 19 -s 2 -e 2 -l „-i shortreadcontigs.fa -L3000 -A“
```

Similarly, we assembled *S. vitreus*, using the *S. lucioperca* contigs and *P. flavescens* chromosomes as references for chromosomal assembly. Here, the short-read contigs were treated as long-reads:

```
CSA2.6c.pl -r longreads+contigs.fa.gz -g sanLuc.CTG.fa.gz,PFLA_1.0_genomic.fna.gz -k 19 -s 2 -e 2
```

The assemblies were manually curated, and the consensus sequences were polished using long reads and flye (v2.6) [39], with options: --nanoraw --polish-target, followed by two rounds of polishing by Pilon (v1.23) [30], using the short-read data, which had been mapped by Minimap2 (v2.17-r941) [27], to the genome assemblies.

Genome annotation

De novo repeat annotation was performed using RepeatModeler (version open-1.0.8) and Repeat Masker (version open-4.0.7). The *P. fluviatilis* genome has been assigned to the RefSeq assembly section of NCBI and has been annotated by GNOMON (www.ncbi.nlm.nih.gov/genome/annotation_euk/process), which included evidence from Actinopterygii proteins (n=154,659) and *P. fluviatilis* RNAseq reads (n = 3,537,868,978) ([www.ncbi.nlm.nih.gov/genome/annotation_euk/Perca fluviatilis/100](http://www.ncbi.nlm.nih.gov/genome/annotation_euk/Perca_fluviatilis/100)). To annotate our *P. schrenkii* and *S. vitreus* assemblies, we used the high-quality GNOMON annotations from their closest relatives *P. flavescens* ([www.ncbi.nlm.nih.gov/genome/annotation_euk/Perca flavescens/100](http://www.ncbi.nlm.nih.gov/genome/annotation_euk/Perca_flavescens/100)) and *S. lucioperca* ([www.ncbi.nlm.nih.gov/genome/annotation_euk/Sander lucioperca/101](http://www.ncbi.nlm.nih.gov/genome/annotation_euk/Sander_lucioperca/101)), respectively. We performed high-throughput comparative protein coding gene annotation by spliced alignment of GNOMON mRNAs and proteins by Spaln (v2.06f, [40]) to our assemblies and combined the resulting CDS- and UTR-matches into complete gene models by custom scripts. All annotations were benchmarked using BUSCO [41] with the Actinopterygii_odb9 database and obtained highly similar values as the reference annotations used for the comparative annotation approach.

Genome browsers and data availability

We provide UCSC genome browsers [42] for the five available *Perca* and *Sander* reference genomes (this study: *P. fluviatilis*, *P. schrenkii*, *S. vitreus*; earlier studies: *P. flavescens* [9] and *S. lucioperca* [22] at <http://genomes.igb-berlin.de/Percidae/>. These genome browsers provide access to genomic sequences and annotations (either public NCBI GNOMON annotations or annotations resulting from our comparative approach). Blat [43] servers for each genome are available to align nucleotide or protein sequences.

Phylogenomics and divergence time estimation

We performed pair-wise whole-genome alignments of 36 teleost genome assemblies as in [44], using Last-aligner and Last-split [45] for filtering 1-to-1 genome matches, Multiz [46] for multiple alignment construction from pairwise alignments and filtered for non-coding sequences to calculate the species tree using iqtree2 and raxml-ng [47,48]. We added the genomes of *P. schrenkii*, *S. vitreus* and *Etheostoma spectabile* (GCF_008692095.1) to this dataset and re-analyzed the highly-supported subclade containing Percidae species using several outgroups (*Lates*, *Oreochromis*, *Pampus* and *Thunnus* sp.). We estimated divergence times using a large subset of our multiple alignment (10^6 nt residues) and the approximate method of Mctree (Paml package version, [49]). We calibrated 5 nodes of the tree by left or right CI values, obtained from www.timetree.org and applied independent rates or correlated rates clock models and the HKY85 evolutionary model. Approximately 10^8 samples were calculated, of which we used the top 50% for divergence time estimation. Each calculation was performed in two replicates, which were checked for convergence using linear regression. The final tree was plotted using FigTree (v1.4.4, <http://tree.bio.ed.ac.uk/software/figtree>).

Perca fluviatilis RAD-Sequencing

Perca fluviatilis gDNA samples from 35 males and 35 females were extracted with the NucleoSpin Kit for Tissue (Macherey-Nagel, Duren, Germany), following the manufacturer's instructions. Then, gDNA concentrations were quantified with a Qubit3 fluorometer (Invitrogen, Carlsbad, CA) using a Qubit dsDNA HS Assay Kit (Invitrogen, Carlsbad, CA). RAD libraries were constructed from each individual's gDNA, using a previously described protocol with the single *Sbf1* restriction enzyme [50]. These libraries were sequenced on an Illumina HiSeq 2500. Raw reads were demultiplexed using the process_radtags.pl wrapper script of stacks, version 1.44, with default settings [51], and further analyzed with the RADSex analysis pipeline [52] to identify sex-specific markers.

Perca fluviatilis Pool-Sequencing

Sequencing of pooled samples (Pool-Seq) was carried out in *Perca fluviatilis* to increase the resolution of RAD-Sequencing for the identification of sex-specific signatures characteristic of its sex-determining

region. The gDNA samples used for RAD-Sequencing were pooled in equimolar quantities according to their sex. Pooled male and pooled female libraries were constructed using a Truseq nano kit (Illumina, ref. FC-121-4001) following the manufacturer's instructions. Each library was sequenced in an Illumina HiSeq2500 with 2x 250 reads. Pool-Seq reads were analyzed as previously described [9,11,53–55] with the PSASS pipeline (psass version 2.0.0: https://zenodo.org/record/2615936#.XtyIS3s6_AI) that computes the position and density of single nucleotide variations (SNVs), heterozygous in one sex but homozygous in the other sex (sex-specific SNVs), and the read depths for the male and female pools along the genome to look for sex coverage differences. Psass was run with default parameters except –window-size, which was set to 5,000, and –output-resolution, which was set to 1,000.

PCR-based sex diagnostics

A *Perca schrenkii* PCR-based sex-diagnostic test was designed based on multiple alignments of the different *amhr2* genes in *P. fluviatilis* (one autosomal gene only), *P. flavescens* (two genes), and *Perca schrenkii* (two genes) to target a conserved region for all *Perca amhr2* genes, allowing the design of PCR-primers that amplify both the autosomal *amhr2a* and the male-specific *amhr2bY* with different and specific PCR-amplicon sizes. Selected PCR primer sequences were forward: 5'-AGTTTATTGTGTTAGTTTGGGCT-3' and reverse: 5'-CAAATAAATCAGAGCAGCGCATC-3'. PCRs were carried out with 1U Platinum Taq DNA Polymerase and its corresponding Buffer (Thermofisher) supplemented with 0.8 mM dNTPs (0.2mM each), 1.5 mM MgCl₂ and 0.2 μM of each primer with the following cycling conditions, 96°C for 3 min; 40 cycles of denaturation (96°C, 30 s), annealing (54°C, 30 s) and extension (72°C, 1 min); final extension (72°C, 5 min); storage at 4°C. PCR amplicons were separated on 1.5% agarose gels (1.5% std. agarose, 1x TBE buffer, 5 V/cm, running time 40 min) and the systematic amplification of the autosomal (*amhr2a*) amplicon was used as a positive PCR control.

Perca fluviatilis primers were designed to amplify a 27 bp-deletion variant in the third intron of the *P. fluviatilis hsd11* gene, which was identified as a male specific (Y-specific) variation based on the pool-seq analysis. Selected PCR-primer sequences were forward 5'-ACACTGATCAACATTTTCTGTCTCA-3' and reverse 5'-TGTTAACATTTGAGAATTTTGCCTT-3'. PCRs were carried out as described above with the following cycling conditions: denaturation 96°C for 3 min; 40 cycles of denaturation (96°C, 30 s), annealing (60°C, 30 s) and extension (72°C, 30 min); final extension (72°C, 5 min); storage at 4°C. PCR amplicons were separated on 5% agarose gels (5% Biozym sieve 3:1 agarose, 1x TBE buffer, 5 V/cm, 1 h 40 min running time) and the amplicon derived from the amplification of the X-chromosome allele was used as a positive PCR control. In addition to this classical PCR sex-genotyping method, we also explored the sex-linkage of some sex-specific SNVs in *P. fluviatilis* using Kompetitive Allele-Specific Polymerase chain reaction (KASPar) assays [56]. Seven sex-specific SNVs were selected at different locations within the *P. fluviatilis* sex-determining region. Primers (Table 1) were designed using the

design service available on the 3CR Bioscience website (www.3crbio.com/free-assay-design). KASPar genotyping assays were carried out with a single end-point measure on a Q-PCR Light Cycler 480 (Roche) using the Agencourt® DNAdvance kit (Beckman), following the manufacturer's instructions.

RNAseq expression analyses

Already available gonadal datasets of *P. fluviatilis* (age 9 month) RNAseq [57] (SRA accessions: SRR14461526 and SRR14461527) were used to compare gene expression between ovary and testes for the gene models annotated in the SD-region. Reads were mapped to our *P. fluviatilis* reference genome using HISAT2 [58] and transcript assembly and FPKM-values were calculated using STRINGTIE [59].

RESULTS

Genome assemblies of Perca fluviatilis, Perca schrenkii and Sander vitreus

The genome of *P. fluviatilis* was sequenced to high coverage using Oxford Nanopore long-read sequencing (estimated coverage: 67-fold / N50 read length: 11.9 kbp), Hi-C data was generated to allow for chromosome-level assembly (coverage: 52-fold / alignable pairs 89.1% / Hi-C map see Suppl. Fig. 1). The final assembly yielded a highly complete reference genome (99.0% of sequence assigned to 24 chromosomes (N50 length: 39.6 Mbp) and highly continuous contigs (N50 length: 4.1 Mbp). Compared to a previously published genome assembly of *P. fluviatilis*, obtained from "linked-short-reads" (10X Genomics), these numbers represent a 316-fold improvement of contig continuity and a 6.3-fold increase of scaffold continuity. The better continuity resulted in an increased percentage of predictable genes (BUSCO results below). Genome assembly statistics are also highly congruent with the previously published reference quality *P. flavescens* genome, except for obvious size differences as the *P. fluviatilis* assembly is about 8.1% larger than the *P. flavescens* assembly and represents the largest genome known in the genus *Perca* (Table 2).

The genome of *P. schrenkii* was assembled by a hybrid assembly method, which was highly efficient regarding long-read sequencing coverage and read length needed (here only 30-fold / N50 read length: 4.95 kb). *De novo* assembled contigs from short reads were combined with long reads and scaffolded using our CSA-pipeline [38], with the *P. flavescens* as the closest reference genome (Fig. 1: divergence time about 7.1 Mya) for genome comparison and inferring chromosomal-level sequences. Using this approach, we were able to assemble the genome of *P. schrenkii* to similar quality as those obtained for *P. flavescens* and *P. fluviatilis* (94.7% assigned to 24 chr. / contig N50 length: 3.2 Mbp; Table 2). The

genome assembly size of *P. schrenkii* was in between the other two *Perca* sp. genomes (877 Mbp < 908 Mbp < 951 Mbp).

The genome of *Sander vitreus* was assembled from long reads (coverage: 12-fold / N50 read length: 10 kb) and short reads similar to procedures for *P. schrenkii* but we used two reference genomes for chromosomal assembly. First, contigs of *S. lucioperca* (closest relative, divergence time 9.8 Mya) served to order the *S. vitreus* contigs (N50: 6.2 Mb), which improved scaffold N50 significantly (result. N50: 16.8 Mb), then these nearly chromosome-scale scaffolds were ordered according to the *P. flavescens* (div. time 19.1 Mya) Hi-C chromosomes (result. N50: 33.3 Mb / 96.5% assigned to 24 chromosomes). This two-step approach resulted in more consistent results than just using the *S. lucioperca* chromosomal scaffolds, which were generated by genetic linkage mapping. We observed similar genome size differences as in *Perca* sp. between both *Sander* species. The *S. vitreus* genome assembly (791 Mb) is smaller than the one of *S. lucioperca* (901 Mb), thus the North American *Sander* and *Perca* species tend to have smaller genome sizes than their Eurasian relatives (Table 2).

De novo repeat analysis showed that 60.1% of the genome assembly size difference between *Sander vitreus* and *S. lucioperca* could be explained by repeat expansion/reduction. Similarly, for *Perca flavescens* and *P. fluviatilis* about 64.8% of the genome size differences were due to repeat expansion/reduction. In both species pairs most repeat expansions/reductions were observed in repeat elements classified as “unknown”. Regarding annotated repeat element classes, L2, DNA, Helitron, CMC-EnSpm, hAT, Rex-Babar, hAT-Charlie and PiggyBac elements expanded the most in both Eurasian species (together adding roughly 20 Mbp to the genomes of *S. lucioperca* and *P. fluviatilis*), while a clear expansion of only a single repeat element, called RTE-BovB, was found in both North American species (adding about 3 and 7 Mbp of sequence to *S. vitreus* and *P. flavescens*, respectively; Suppl. table 1).

The genome of *P. fluviatilis* was annotated by NCBI/GNOMON, which included ample public RNAseq data and protein homology evidence. For *P. schrenkii* and *S. vitreus*, we transferred the NCBI/GNOMON annotations of *P. flavescens* and *S. lucioperca*, respectively. BUSCO analysis (Table 3) revealed values larger than 95.9% for complete BUSCOs (category “C:”) for all annotations. The comparative annotation approach resulted only in small losses (category “M:”) of a few BUSCO genes in the range of 0.4% - 1.1%. In this regard, the *S. vitreus* assembly performed better than the *P. schrenkii* assembly, possibly due to the higher N50 read length of the underlying long-read data.

***Percomorpha* phylogenomics and divergence time estimation**

To calculate the phylogenetic tree of 36 *Percomorpha* species and their divergence times, we aligned whole genomes and extracted the non-coding alignments (Fig. 1). The use of non-coding sequences is

preferable to calculate difficult-to-resolve phylogenetic trees that occur after massive radiations [60–62]. Our multiple alignment consisted of 6,594,104 nt residues (2,256,299 distinct patterns; 1,652,510 parsimony-informative; 1,136,496 singleton sites; 3,805,098 constant sites) and resulted in a highly-supported tree (raxml-ng and IQtree2 topologies were identical; all IQtree2's SH-aLRT and ultrafast bootstrapping (UFBS) values were 100). According to the divergence time analysis, most Percomorpha orders emerged after the Cretaceous–Paleogene (K-Pg) boundary about 65.9 Mya ago (CI: 51.3 - 83.6). The lineage leading to the Percidae (represented with species of *Perca*, *Sander*, and *Etheostoma*) emerged about 58.9 Mya (CI: 45.8 - 74.2), and the extant Percidae species analyzed in this study diverged from a last common ancestor (LCA) about 26.9 Mya (CI: 16.8 - 43.4). The *Perca* and *Sander* genera split about 19.1 Mya (CI: 11.8 - 31.1), and *S. vitreus* and *S. lucioperca* splitted at 9.8 Mya (CI: 5.7 - 18.9) similar to the divergence of *P. fluviatilis* from *P. flavescens* and *P. schrenkii* 10.9 Mya (CI: 7.1 - 18.6). The closest *Perca* species are *P. flavescens* and *P. schrenkii* which diverged about 7.1 Mya (CI: 4.2 - 11.4), although today both species are occurring in completely different global ranges.

The fate of amhr2 genes during evolution of Perca and Sander species

In the genome of *P. flavescens*, two *amhr2* paralogs were previously described, i.e., an autosomal gene, *amhr2a*, present in both males and females on chromosome 04 (Chr04), and a male-specific duplication on the Y-chromosome (Chr09), *amhr2bY* [9]. A similar *amhr2* gene duplication was also found in our male *P. schrenkii* assembly, and sequence homologies and conserved synteny analyses show that these two *P. schrenkii* *amhr2* genes are orthologs of *P. flavescens* *amhr2a* and *amhr2bY*, respectively (Fig. 2A and AB). Genotyping of one male and one female also suggests that the *amhr2bY* gene could be male-specific in *P. schrenkii* (Suppl. Fig. 2, Table 4), as described in *P. flavescens* [9]. This potential sex-linkage is also supported by a half coverage of reads in the genomic region containing the *amhr2bY* locus in our male *P. schrenki* genome assembly (Suppl. Fig. 3), in agreement with the hemizyosity of a male-specific region on the Y in species with a XX/XY sex determination system. Alignment of the *P. schrenkii* *amhr2bY* ortholog shows that its coding sequence (CDS) shares 98% identity with the *P. flavescens* *amhr2bY* CDS and 95.7 % identity at the protein level the *P. flavescens* *Amhr2bY*. As in *P. flavescens* [9], the *P. schrenkii* *amhr2bY* gene encodes a N-terminal-truncated type II receptor protein that lacks most of the cysteine-rich extracellular part of the receptor, which is crucially involved in ligand-binding specificity [63] (Fig. 3).

In contrast, in our *P. fluviatilis* male genome assembly, only one copy of *amhr2* could be identified and sequence homologies and conserved synteny analysis (Fig. 2A and 2B) shows that this *amhr2* gene is the ortholog of *P. flavescens* and *P. schrenkii* *amhr2a*. In addition, PCR with primers designed to amplify both *amhr2a* and *amhr2bY* from *P. flavescens* and *P. schrenkii* did not show any sex-differences in *P. fluviatilis*. Altogether, these results support the absence of an *amhr2b* gene in *P. fluviatilis*.

In the *Sander lucioperca* male genome assembly, four copies of *Amhr2* were detected. Using the same primers as those used for the amplification of both *amhr2a* and *amhr2bY* in *P. flavescens* and *P. schrenkii*, PCR genotyping on males and females of *S. lucioperca* produced complex amplification patterns with multiple bands and no visible association with sex. In the publicly available genome assembly of *Sander vitreus*, sequence homologies and /or conserved synteny analysis (Fig. 2A and 2B) allowed the identification of a single autosomal *amhr2a* gene.

A phylogenetic analysis of the sequences with similarity to *amhr2* in *Perca* and *Sander* (Fig. 2A and 2B) shows that the different *amhr2* genes likely originated from a gene duplication event that happened in the branch leading to the last common ancestor of these species, dated around 19-27 Mya. Since that time, the *amhr2bY* gene has been conserved in *P. schrenkii* and *P. flavescens*, lost in *P. fluviatilis* and *S. vitreus*, and amplified in *S. lucioperca*.

Evolution of sex determination in P. fluviatilis

Because *P. fluviatilis* sex determination does not rely on an *amhr2* duplication like what has been found in *P. flavescens* [9] and *P. schrenkii* (this study), we used genome-wide approaches to better characterize its sex-determination system. RAD-Seq analysis on 35 males and 35 females of *P. fluviatilis*, carried out with a minimum read depth of one, allowed the characterization of a single significant sex marker (Suppl. Fig. 4). This 94 bp RAD sequence matches (Blast Identities: 93/95%) a portion of *P. fluviatilis* chromosome 18 (GENO_Pfluv_1.0, Chr18: 27656212 - 27656305). This RAD-Seq analysis suggests that Chr18 could be the *P. fluviatilis* sex chromosome, and that its sex-determining region could be very small because we only detected a single significant sex-linked RAD-sequence. To get a better characterization of the *P. fluviatilis* sex chromosome and sex-determining region, we then used Pool-Sequencing (Pool-Seq) to re-analyze the same samples used for RAD-Seq by pooling together DNA from the males in one pool and DNA from females in a second pool. Using these Pool-Seq datasets, we identified a small 100 kb region on *P. fluviatilis* Chr18 with a high density of male-specific SNVs (Fig. 4), confirming the RAD-Seq hypothesis that Chr18 is the sex chromosome in that species. No male-specific duplication / insertion event was found in this sex-determining region on Chr18, which contains six annotated genes (Fig. 4D). These genes encode a protein of unknown function (*C18h1orf198*), three gap-junction proteins (*Cx32.2*, *Gja13.2* and *Cx32.7*), a protein annotated as inactive hydroxysteroid dehydrogenase-like protein (*Hsd11*), and a protein known as protein broad-minded or Tcb1 domain family member 32 protein (*Tbc1d32*). Three of these six annotated genes, i.e., *c18h1orf198*, *hsd11* and *tbc1d32* display a higher expression in testis than in the ovary (Suppl. Fig. 5).

To provide a better support for the sex-linkage of the male-specific variants found within this sex determining region on Chr18, we designed different types of genotyping assays (classical PCR and

KASpar) that have been applied to different *P. fluviatilis* individuals which were phenotypically sexed with confidence. A classical PCR-assay was first developed based on the detection of a Y-allele-specific 27 bp deletion in the third intron of the *P. fluviatilis* *hsl1* gene, (Suppl. Fig. 6, Table 4) and this assay successfully identified all males of a Lake Mueggelsee from Germany (10 males and 9 females; p-value of association with sex = 9.667e-05). In addition, KASpar allele-specific PCR-assays were developed based on seven single nucleotide sex-specific variants, located at different positions within the Chr18 sex-determining region of *P. fluviatilis* (Fig. 3D). Tests of 48 males and 48 females showed that of seven KASpar allele-specific PCR-assays, five resulted in a high proportion of correctly-genotyped individuals with males being heterozygote and females being homozygote (>95%). Two of the targeted SNVs (SNV1 and SNV3) that displayed 100% sex-linkage accuracy (Suppl. Fig. 7, Tables 4 and 5). Sex-linkage of SNV1 was then checked on a wild-type population from Kortowskie Lake in Poland for which the association of male phenotype and SNV1 heterozygosity was also complete (17 males and 20 females; p-value = 8.83e-09, Table 4).

DISCUSSION

The Percidae family is represented by 239 species and 11 genera. The genera *Perca* and *Sander* are especially important for aquaculture and fisheries. By providing new genome sequence assemblies for *Perca fluviatilis*, *P. schrenckii* and *Sander vitreus*, we provide for the first-time access to all economically important species of the *Percidae* at the DNA-level. Assembly statistics for these three new genome sequence assemblies are reference grade with N50 continuity in the megabase range and chromosomal length scaffolds, obtained either by Hi-C scaffolding or by conserved synteny analysis involving the closest relatives. Importantly completeness on the gene-level is significantly higher than in a short-read based draft genome for *P. fluviatilis*, published earlier [64], allowing much stronger conclusions to be drawn regarding the presence or absence of possible sex-determining genes.

The origin of Percidae

A phylogenomic approach using aligned non-coding sequences of 36 genomes resulted in a highly-supported tree showing a rapid radiation of fish families. It has recently been shown that phylogenomics based on non-coding sequences may be more reliable at resolving difficult-to-resolve radiations in species trees (i.e. in Aves). According to our time calibration, many taxonomic orders related to the Percidae emerged shortly after the Cretaceous-Paleogene (K-Pg) mass extinction event, about 66 Mya, and gave rise to Percidae about 59 Mya. This is in contrast to many older studies, which have, for example, dated the split of *Perca ssp.* and *Gasterosteus ssp.* back to the Cretaceous (73-165 Mya; 18 of 23 studies listed at www.timetree.org). Similar patterns in rapid radiations have been

observed in the avian tree of life and have likewise been attributed to the K-Pg mass extinction [61,62]. In context, it has been argued that the so-called “Lilliput effect”, which describes the selection in favor of species with small body sizes and fast generation times after mass extinction events, can lead to an increase in substitution rates and results in overestimations of node-ages for molecular clocks [65].

The evolution of sex determination in *Perca* and *Sander* species

Evolution and turnover of *Amhr2*

Sex determination systems with MSD evolved from duplications of the *amh* [10–17] or *amhr2* [9,18–21] genes have now been characterized in many fish species, all with a male-heterogametic system (XX/XY). In addition, the fact that *Amh* in monotremes [66], or *Amhr2* in some lizards [67] are Y-linked also makes them strong MSD gene candidates in other vertebrate species. In Percidae, sex determination has only been explored in some species of *Perca* [8,9], and *Amhr2* has been characterized as a potential MSD gene in yellow perch, *P. flavescens* [9]. Our results suggest that this duplication of *amhr2* in *P. flavescens* is also shared by *P. schrenkii* and *S. lucioperca*, implying an origin of duplication in their last common ancestor, dated around 19-27 Mya. However, the fate of this duplication seems to be complex - with multiple duplications/insertions on different chromosomes with no clear sex-linkage in *S. lucioperca*, a secondary loss in *P. fluviatilis* and *S. vitreus*, contrasting with a single potentially sex-linked duplication/insertion in *P. schrenkii* and in *P. flavescens*. This finding suggests that the shared ancestral *amhr2b*-duplicated locus (Fig. 2A) might be a jumping locus that has been moving around during its evolution as found for the *sdY* MSD jumping sex locus in salmonids [68,69]. Additional evidence that these *amhr2b* genes originated a single ancestor also rely on the fact that the *Amhr2b* proteins of *P. flavescens* [9], *P. schrenkii* and *S. lucioperca* share a similar gene structure with an N-terminal truncation that results in the absence of the cysteine-rich extracellular part of the receptor. This part of the receptor is known to be crucial for ligand binding [70]. A similar N-terminal truncation of a duplicated *amhr2* was also described in catfishes from the Pangasidae family, where this truncation had been hypothetically linked to a potentially new sex-determination function that lacks ligand dependency [18]. In the genus *Sander*, the situation might be similar to that in *Perca* regarding the changes of the sex-determination systems between species. In *S. lucioperca*, *amhr2b* might still serve as the MSD-gene, but the several recent *amhr2b* duplications have complicated our analysis so far. Similar to *P. fluviatilis*, *S. vitreus* has lost *amhr2b* and likely another factor took over as a potential MSD-gene.

A new sex-specific locus in *P. fluviatilis*

The fact that *P. fluviatilis* sex does not rely on an *amhr2*-duplication like *P. flavescens* [9] and *P. schrenkii* do, indicates that *P. fluviatilis* evolved a completely different and new MSD-gene. Our results

also show that this sex locus on *P. fluviatilis* Chr18 is very small compared to what is observed in many fish species, with a potentially non-recombining size around 100 kb. This locus however is not the smallest SD-locus described in teleost fish: in the pufferfish, *Takifugu rubripes*, the sex locus is limited to a few SNPs that differentiate *amhr2* alleles on the X- and Y -chromosomes [19]. Because we did not find any sign of a sex chromosome-specific duplication/insertion event in the *P. fluviatilis* SDR, this sex locus seems to result from pure allelic diversification and is thus in contrast to *P. flavescens* [9] and probably also *P. schrenkii* (this study). The *P. fluviatilis* sex specific-region on Chr18 contains six annotated genes, which encode a protein of unknown function (*C18h1orf198*), three gap-junction proteins (*Cx32.2*, *Gja13.2* and *Cx32.7*), a protein annotated as inactive hydroxysteroid dehydrogenase-like protein (*Hsd1l*) and a protein known as protein broad-minded or Tcb1 domain family member 32 protein (*Tbc1d32*). Of these genes, *hsd1l* and *tbc1d32* are interesting potential MSD candidates in *P. fluviatilis*, based on their potential functions and the fact that both display a higher testicular expression compared to the ovary. The *Hsd1l* protein is indeed annotated as “inactive” [71], but this annotation only refers to its lack of enzymatic activity against substrates so far tested, leaving other potential functional roles for a protein that is highly conserved in vertebrates [71]. In *Epinephelus coioides*, *hsd1l* has been shown to be differentially expressed during female-to-male sex-reversal, and its expression profile clustered with *hsd17b1* [72], which plays a central role in converting sex steroids and has recently been identified as a potential MSD gene in different species with a female heterogametic (ZZ/ZW) sex determination system, like in oyster pompano, *Trachinotus anak* [73] and different amberjack species [74,75]. The *Tbc1d32* protein has been shown to be required for a high Sonic hedgehog (*Shh*) signaling in the mouse neural tube [76]. Given the role of *Shh* signaling downstream of steroidogenic factor 1 (*nr5a1*) for the proper steroidogenic lineage fate [77] and the importance of steroids in gonadal sex differentiation [78,79], *tbc1d32* would be also an interesting candidate as a potential MSD gene in *Perca fluviatilis*.

CONCLUSIONS

Our study shows that *Percidae* exhibit a remarkable high variation in sex-determination mechanisms. This variation is connected to deletion or amplification of *amhr2bY*, which if lost in certain species (like *Perca fluviatilis* or *Sander vitreus*) should cause re-wiring of the sex determining pathways and result in the rise of new SD-systems. The mechanisms behind a “jumping” *amhr2bY* expansion or loss and which genes replace it as the MSD remain to be elucidated. The new *Percidae* reference sequence assemblies presented here and the highly reliable sex markers developed for *P. fluviatilis* can now be applied for sex genotyping in basic science as well in aquaculture.

518 **DATA AVAILABILITY**

519 All genome assemblies and raw sequence datasets have been submitted to NCBI/GENBANK under the
520 bioproject accessions: PRJNA549142, PRJNA637487, PRJNA808842 (*P. fluviatilis*, *P. schrenkii*, *S. vitreus*,
521 respectively).

522 **BENEFIT-SHARING STATEMENT**

523 A research collaboration was developed with scientists from the countries providing genetic samples
524 (PE and WL in USA, DZ in Poland and ST in Russia), all collaborators are included as co-authors, the
525 results of research have been shared with the provider communities, and the research addresses a
526 priority concern, in this case the conservation of organisms being studied. More broadly, our group is
527 committed to international scientific partnerships, as well as institutional capacity building.

528 **ACKNOWLEDGEMENTS**

529 We kindly acknowledge the NCBI/Genbank team for providing a GNOMON annotation of the *P.*
530 *fluviatilis* genome. This work was funded by the German Research Foundation (DFG) “Eigene Stelle”
531 grant KU 3596/1-1; project number: 324050651, by the Agence Nationale pour la Recherche (ANR) /
532 DFG PhyloSex project (ANR-13-ISV7-0005), the CRB-Anim “Centre de Ressources Biologiques pour les
533 animaux domestiques” project PERCH'SEX, the FEAMP “Fonds européen pour les affaires maritimes et
534 la pêche” project SEX'NPERCH, NIH (R35 GM139635), and NSF (2232891). The GeT-PlaGe and MGX
535 sequencing facilities were supported by France Génomique National infrastructure as part of the
536 “Investissement d’avenir” program managed by (ANR-10-INBS-09). We thank Dr. Tatjana Dujsebayeva,
537 Salamat Karlybai and his colleague for help during field work in Kazakhstan. We thank Eva Kreuz and
538 Wibke Kleiner for technical assistance. We thank Matt Faust (Ohio, DNR) for help with samples of *S.*
539 *vitreus*.

540 **AUTHOR CONTRIBUTIONS**

541 YG and HK designed the project. PE, WL provided sexed samples of *S. vitreus*. MW, BS, TL, ST, SV, DZ
542 collected and sexed the *P. fluviatilis* samples. MS in collaboration with ST did field work in Kazakhstan,
543 collected and sexed the tissue samples of *P. schrenkii*. EJ, MW, CR, CI, HP and HK extracted the gDNA,
544 made the genomic libraries and sequenced them. CeC, ChK, MZ, MW, ClK, RF, AH, HK and YG processed
545 the genome assemblies and/or analyzed the results. CP, LJ, CaC processed and analyzed the sex
546 genotyping tests. HK and YG wrote the manuscript with inputs from all other coauthors. JHP, CD, HK
547 and YG, supervised the project administration and raised funding. All the authors read and approved
548 the final manuscript.

549 **COMPETING INTERESTS**

550 All authors declare no competing interests.

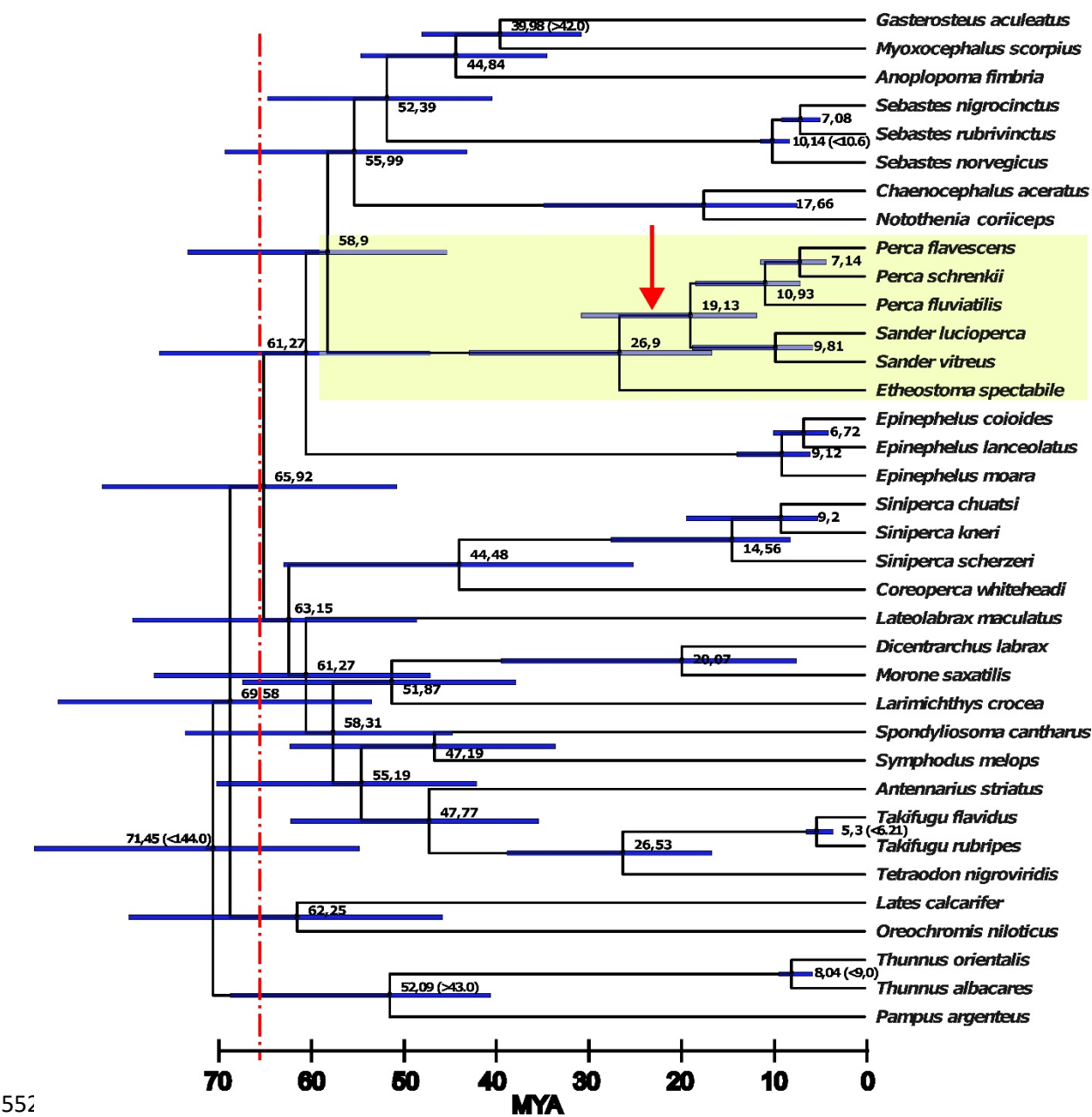


Figure 1: Time calibrated phylogenomic tree constructed from non-coding alignments of 36 *Percomorpha* genome assemblies reveals a massive radiation after the Cretaceous–Paleogene (K–Pg) boundary (66 Mya, dotted red line). The family Percidae is highlighted in yellow. Node numbers depict the median ages in Mya calculated by Mctree (values in brackets were taken from www.timetree.org and used for calibration). Blue bars depict the 95% confidence intervals for the node ages. Red arrow indicates duplication event of *amhr2* in Percidae (more details in Fig. 2a, *amhr2* gene tree). All branches of the tree obtained 100% support using the SH-aLRT (Shimodaira–Hasegawa like approximate likelihood ratio test) and UFBS (ultra-fast bootstrap) tests.

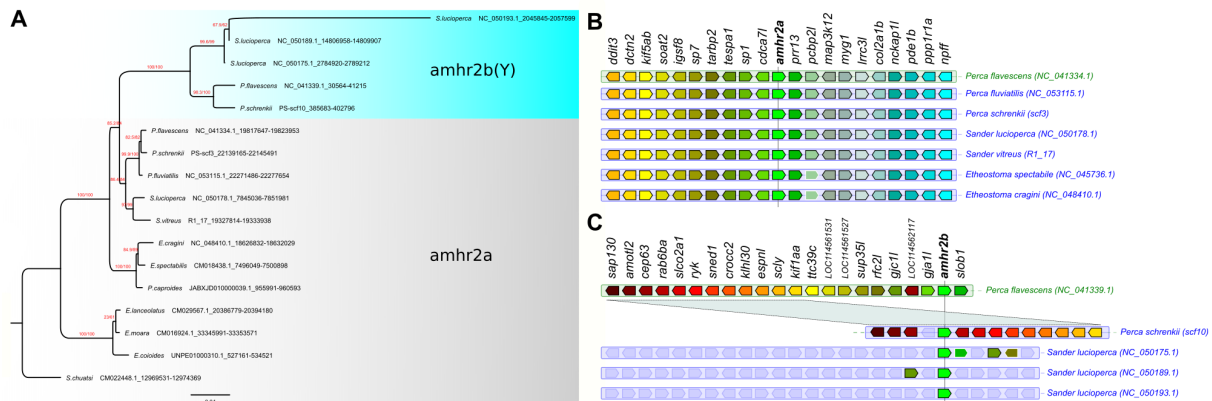


Figure 2: Evolution of *amhr2* genes in Percidae. A. Orthologs of *amhr2a* were identified in genome assemblies and their gene tree is consistent with the species tree, which was found by the phylogenomics approach (see Figure 1) The *amhr2b* duplications were only found in the genome assemblies of *P. flavescens* (single copy, male specific), *P. schrenkii* (single copy, potentially male specific) and *S. lucioperca* (three copies, no clear sex linkage) and they clustered together. Thus, *amhr2b* stems from a gene duplication event that occurred at the origin of Percidae (19-27 Mya) and the absence of *amhr2b* in *P. fluviatilis* and *S. vitreus* suggests a secondary loss event in these species. This tree was calculated on codon position 1 and 2 alignments and achieved the best bootstrap support (red numbers: SH-aLRT / UFBS support values) for the split of the *amhr2a* and *b* clades. Trees based on complete CDS, CDS + Introns and amino acid sequences resulted in the same topology albeit with lower bootstrap support for some splits (Suppl. Fig. 8). Numbers after species names depict the coordinates of the respective *amhr2* genes in the genome assemblies. **B & C. Conserved synteny around the *amhr2a* (B) and *amhr2b* (C) loci in some *Percidae* species.** These multiple duplications (in *S. lucioperca*) or the loss of the *amhr2b* genes (in *P. fluviatilis* and *S. vitreus*) emphasize that *amhr2b* may be considered a “jumping” gene locus, which is also supported by conserved synteny analysis.

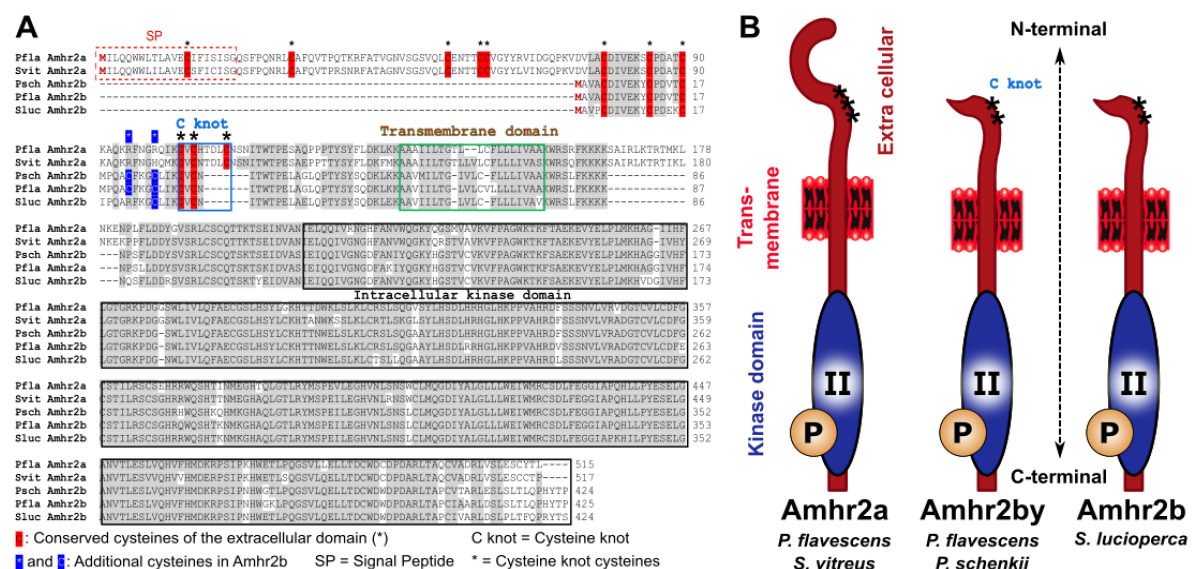


Figure 3: Alignment and structure of Amhr2a and Amhr2b proteins in *Perca flavescens* (Pfla) and *P. schrenkii* (Psch), *Sander lucioperca* (Sluc) and *S. vitreus* (Svit). **A.** Alignment of some Percidae Amhr2a (*P. fluviatilis* and *S. vitreus*) and Amhr2b (*P. schrenkii*, *P. flavescens* and *S. lucioperca*) proteins. **B.** Schematic structure of Amhr2a and Amhr2b proteins.

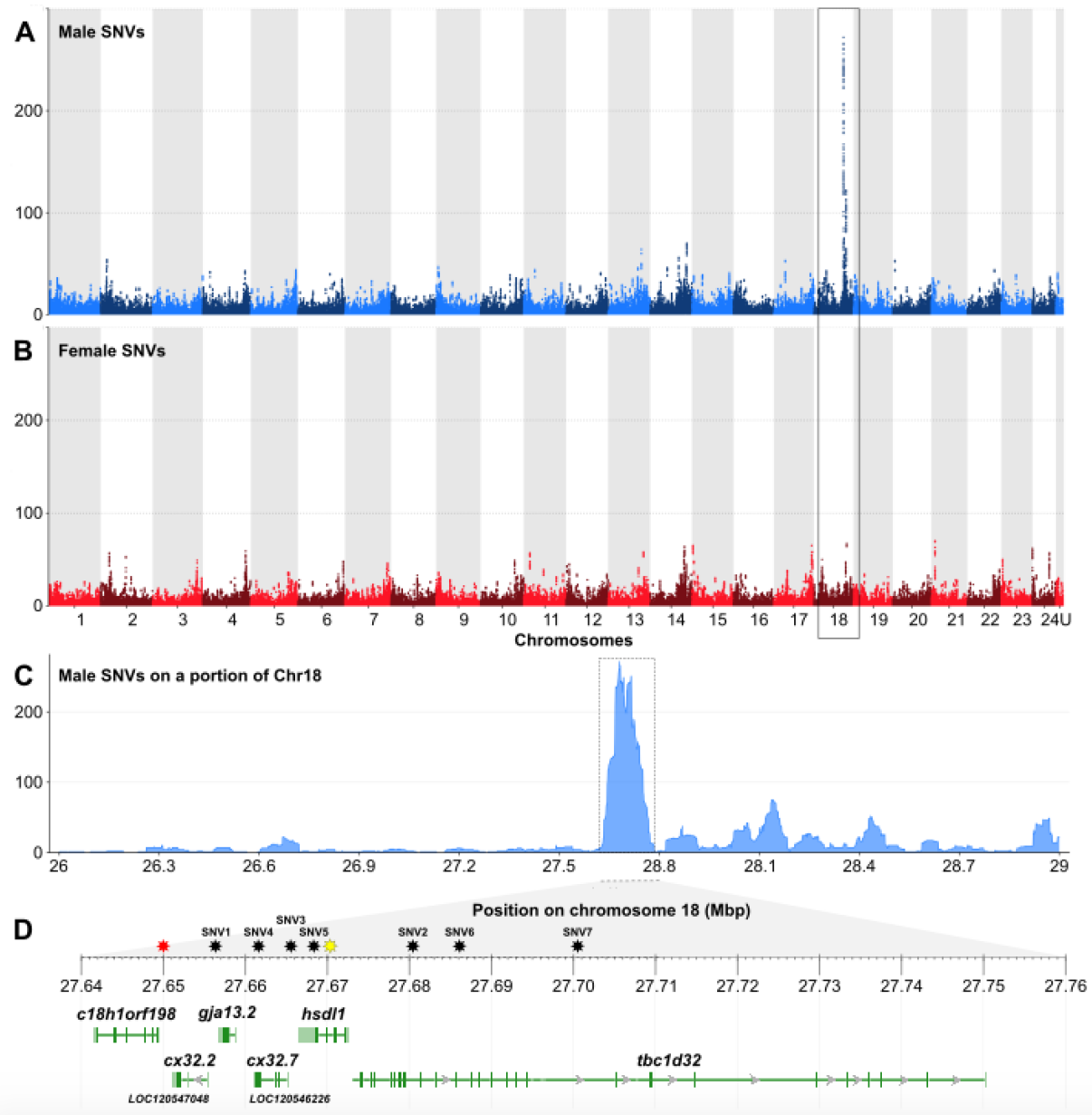
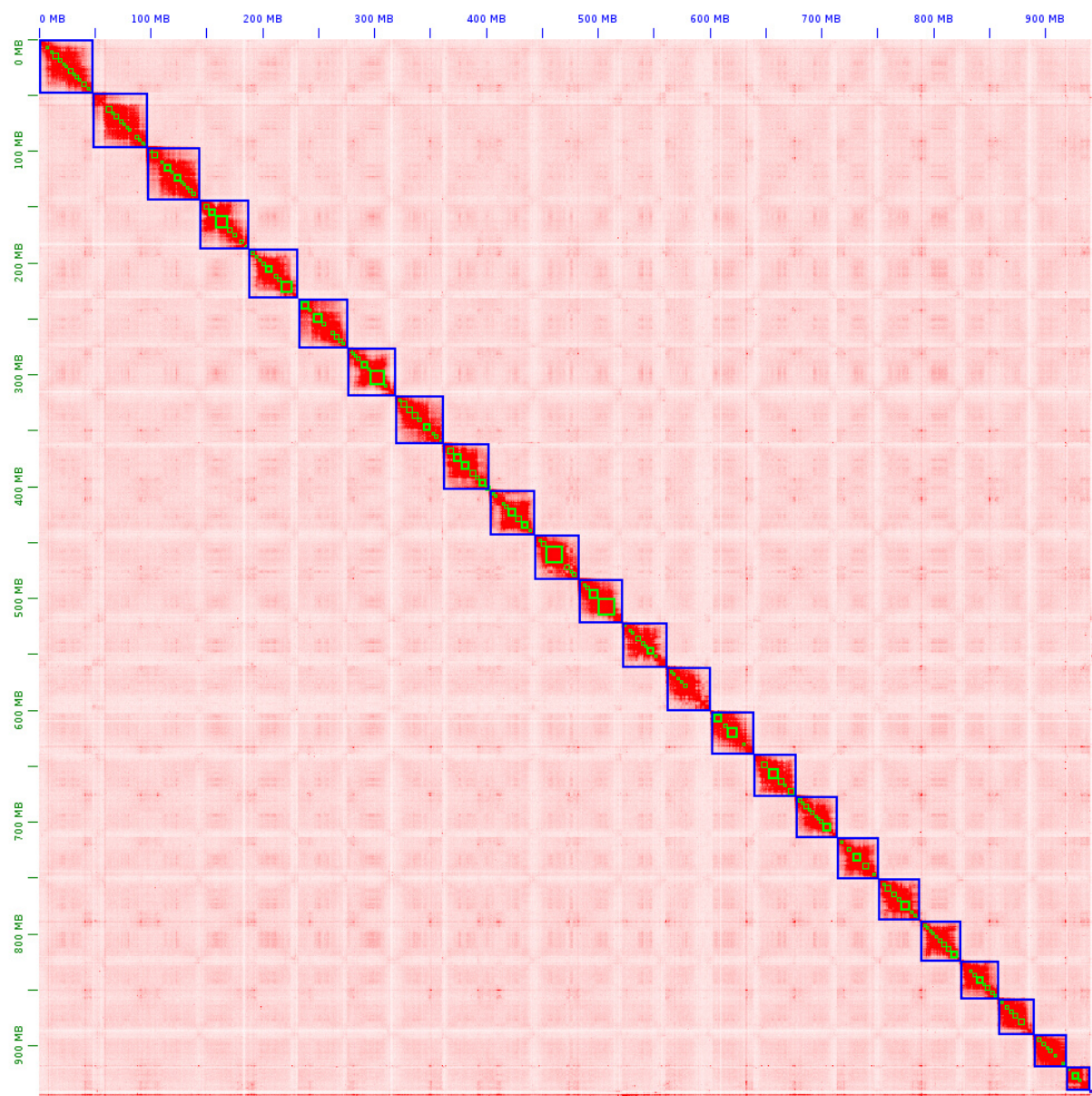


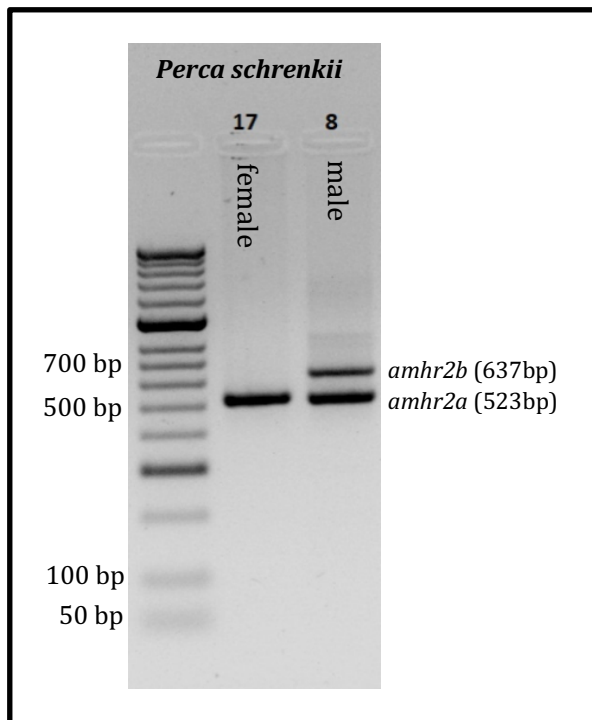
Figure 4: Chromosome 18 is the sex chromosome of *Perca fluviatilis*. (A, B) Genome-wide Manhattan-plots of (A) male- and (B) female- specific single-nucleotide variations (SNVs), showing that chromosome 18 (Chr18) contains a 100 kb region, enriched for male-specific SNVs. Male- and female-specific SNVs are represented as dots (total of SNVs per 50 kb window size) of alternating colors on adjacent chromosomes. (C) Zoomed view of the male-specific SNVs on the sex-biased region of Chr18 with its gene annotation content (D): *c18h1orf198* = *c18h1orf198* homolog ; *cx32.2* (LOC120547048) = gap junction Cx32.2 protein-like ; *gja13.2* = gap junction protein alpha 13.2 ; *cx32.7* (LOC120546226) = gap junction Cx32.7 protein-like ; *hsdl1* = inactive hydroxysteroid dehydrogenase-like protein 1 ; *tbc1d32* = tcb1 domain family member 32 (also known as protein broad-minded). Stars over the ruler of panel D are the locations of the single male-specific RAD maker (red star) and of the SNVs used for designing KASPar assays (black stars; SNV1- 7). The location of the sex-specific intronic indel inside the *hsdl1*-gene used for sex specific PCR is shown by a yellow star



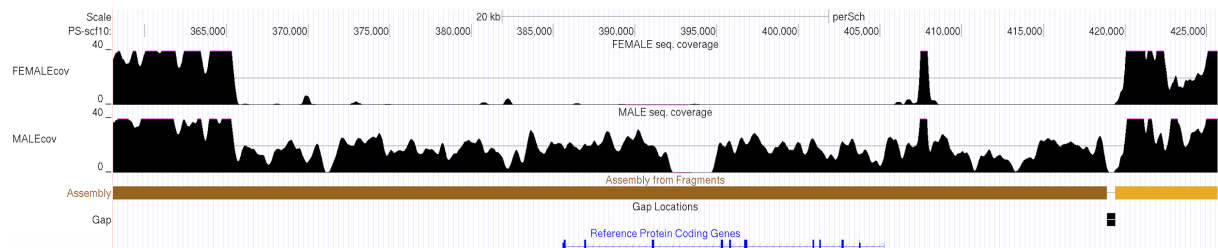
599

600 **Supplementary Figure 1: Hi-C map of *P. fluviatilis* genome.**

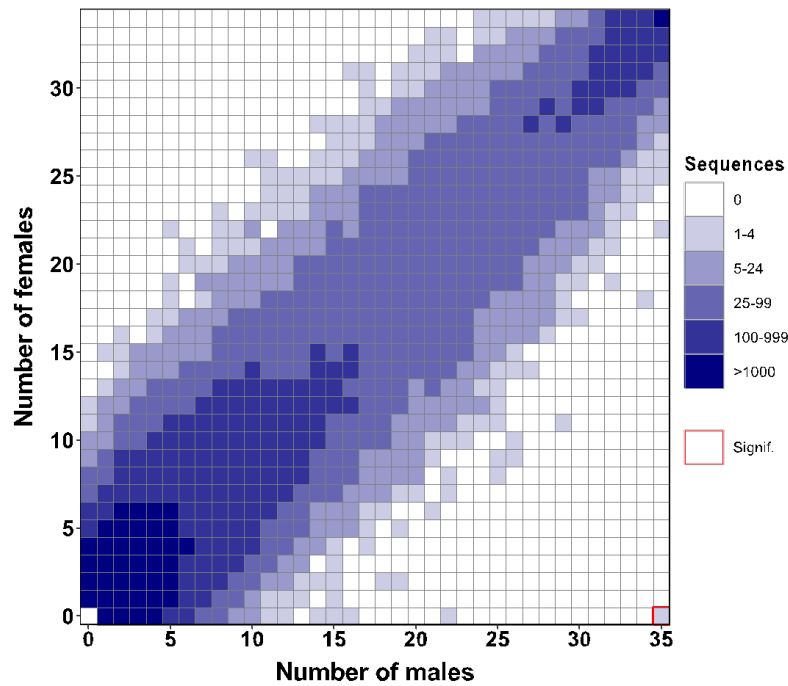
601



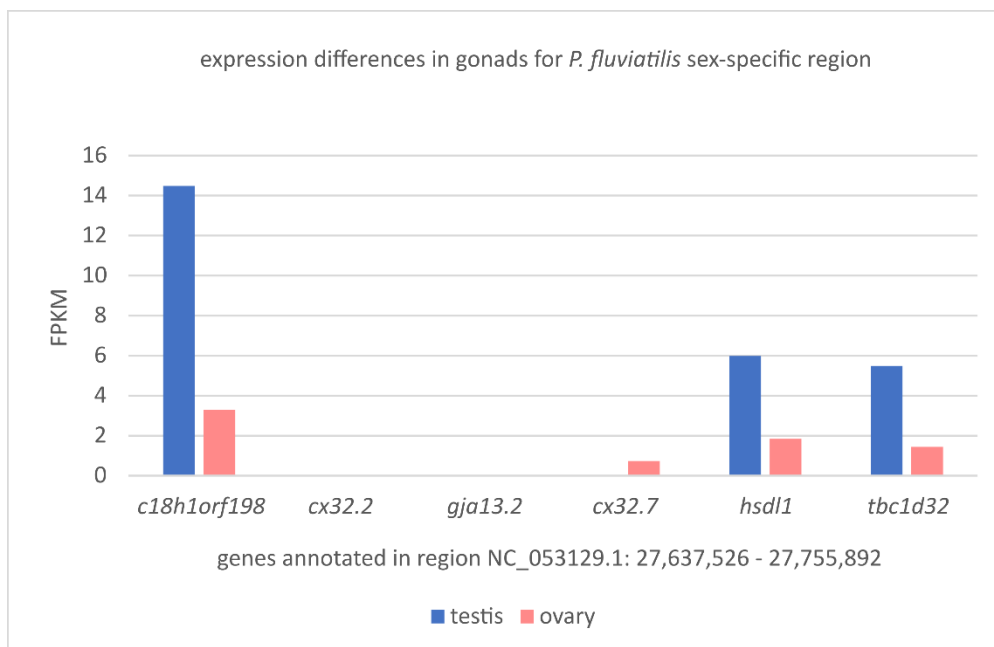
Supplementary Figure 2: A sex-specific 637 bp PCR product amplifies in *P. schrenkii* male (sample id = 8), while it is absent in female (sample id = 17). The corresponding primer pair also works for sexing of *P. flavescens*.



Supplementary Figure 3: Sex-specific sequencing coverage of *amhr2b* locus in *Perca schrenkii* in region PS-scf10 / CM046795.1: 366,025-418,970. A female and a male genome were sequenced to approximately 40x coverage using short-read sequencing. After filtering for unique mapping reads (mapping quality 60), a clear coverage difference between females and males is visible. The ~53 kbp region has virtually no coverage in females. In contrast males exhibit haploid coverage (about 20x), which is in accordance with a X/Y SD system.

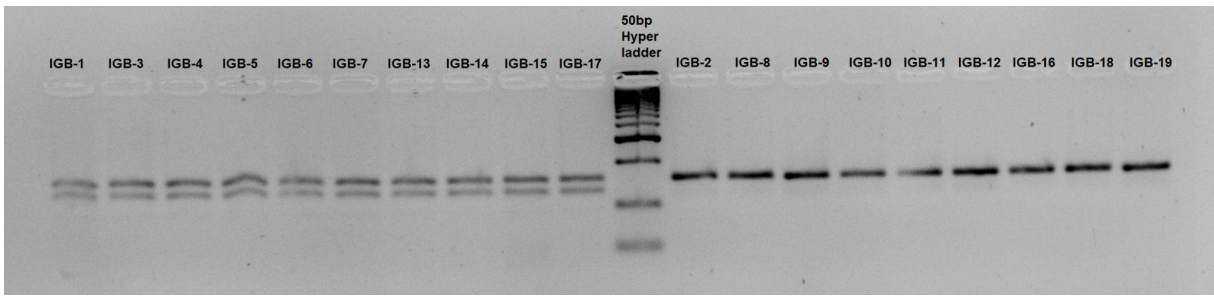


Supplementary Figure 4: A single RAD sex-specific marker is significantly associated with male sex in *P. fluviatilis*. Tile plot of the distribution of RADSex markers between *Perca fluviatilis* males (horizontal axis) and females (vertical axis) with a minimum read depth of 1 ($d = 1$). Color intensity (see color legend on the right) indicates the number of markers present for each of the corresponding number of males and females. A single significant marker at the lower right of the grid was present in all 35 males and absent from all 34 females and is boxed with a red border (Chi-squared test, $p < .05$ after Bonferroni correction).



Supplementary Figure 5: Expression of *hsd11* and neighboring genes in public RNAseq datasets (testis: SRR14461526, ovary: SRR14461527; age of both sampled individuals 9 month). Here *hsd11* expression in testis is 3.25-fold higher than in ovary, for *tbc1d32* and *c18h1orf198* the ratio is 3.83 and 4.41, respectively.

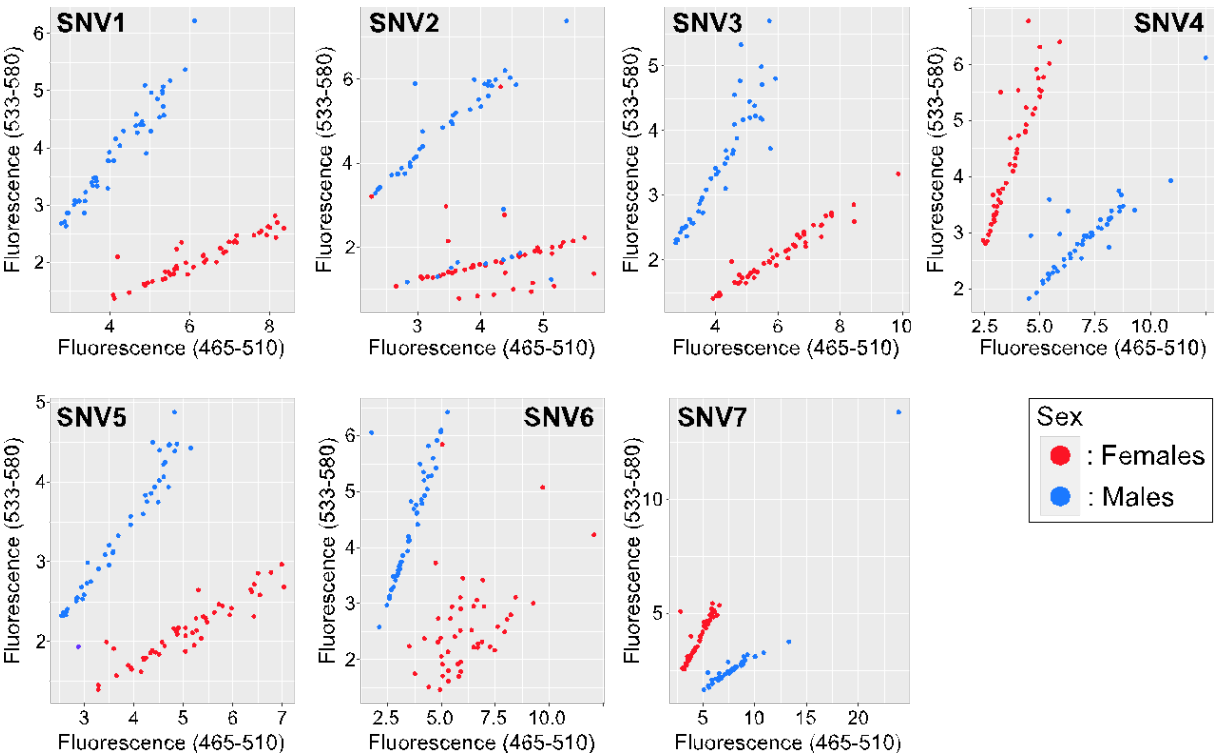
629



630

631 **Supplementary Figure 6:** Sexing of *P. fluviatilis* using a 27 bp male specific deletion in Intron 3 of the *hsl1* gene
632 (10 males (left) and 9 females (right) from Lake Mueggelsee, Berlin. The simultaneous amplification in both males
633 and females of the X allele without the 27 bp deletion provides an internal control for this PCR. All XY male
634 samples (N = 10) produce two amplicons due to the small size difference of the X and Y amplified alleles, and all
635 XX females (N = 9) produced only the larger X amplicon. This *hsl1* intronic indel variant is located near the variant
636 SNV5 (distance < 1.5 kbp).

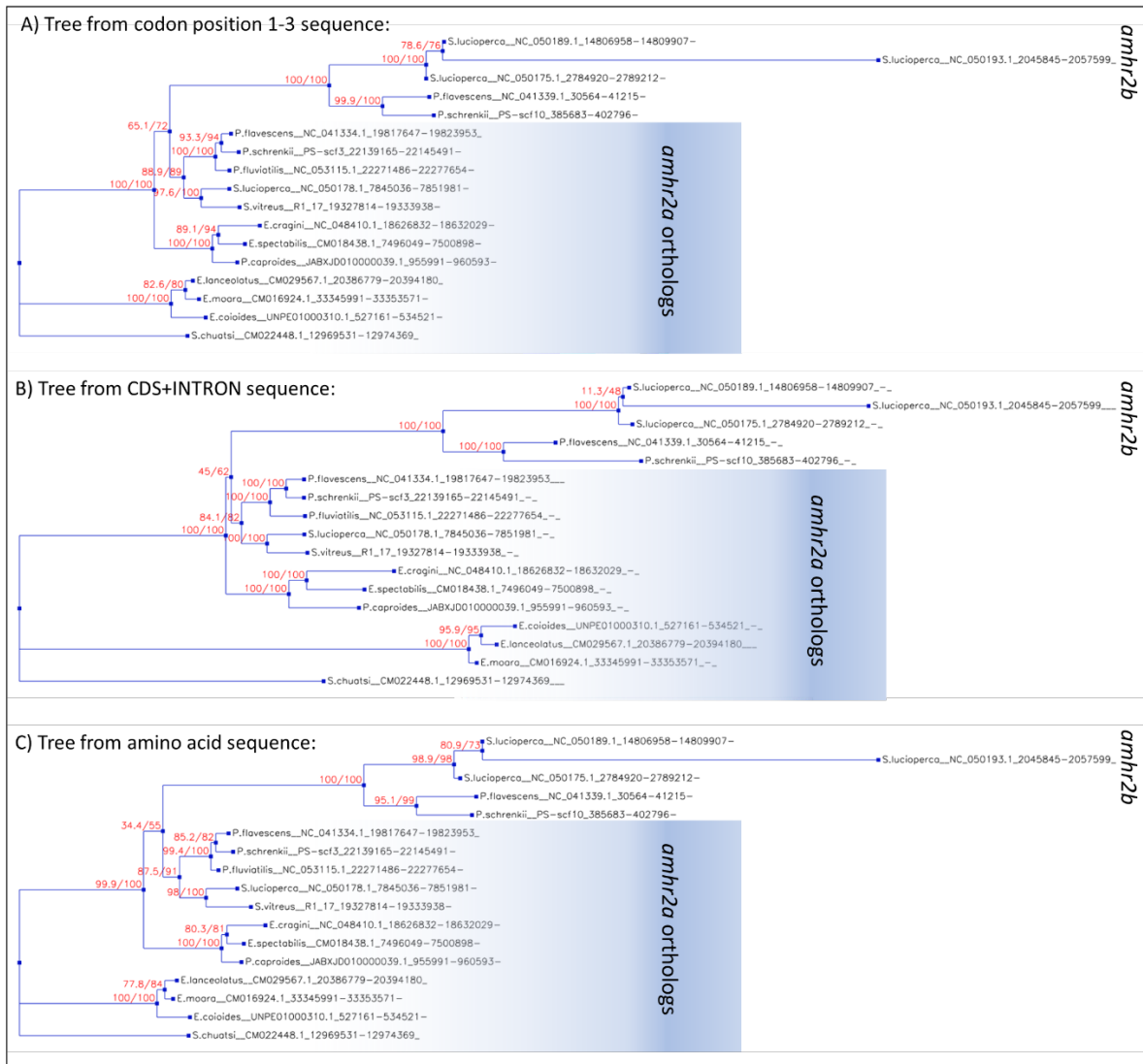
637



638

639 **Supplementary Figure 7:** KASpar allele-specific PCR assays on seven single sex-specific nucleotide
640 variations (SNV ID#) in *P. fluviatilis*. For each Single Nucleotide Variation (SNV), primer AL1 was
641 coupled to FAM fluorescent dye and primer AL2 was coupled to VIC fluorescent dye and the end-point
642 fluorescence of these two fluorescent dyes was respectively on the x- and y- axes. Male individuals are
643 represented by blue dots and females by red dots. Primers used for analysis can be found in Table 1.

644



Supplementary Figure 8: Additional gene trees for *amhr2*. A) Tree calculated from coding sequence. B) Tree calculated from coding plus intron sequence. C) Tree calculated from amino acid sequence. All trees share the same topology but differ in support values for some splits (SH-aLRT and UFBS tests).

TABLES

Table 1: KASpar allele-specific PCR-primers. For each allele (AL1 and AL2) primers, the X and Y sex chromosome-specific alleles are provided along with their sequences.

Primer ID#	Allele (X or Y)	Sequence (5' – 3')
SNV1_AL1	X	GAAGGTGACCAAGTTCATGCTGACACATATTGTCCATCTGATGTAAATG
SNV1_AL2	Y	GAAGGTCGGAGTCAACGGATTATGACACATATTGTCCATCTGATGTAAATT
SNV1_C	Common	CACCACCACTGACTGAAGAATAATATGAA
SNV2_AL1	X	GAAGGTGACCAAGTTCATGCTGGACTGATTGTGCTGCTTCTCTC
SNV2_AL2	Y	GAAGGTCGGAGTCAACGGATTGGACTGATTGTGCTGCTTCTCTT
SNV2_C	Common	CAGATGAGGAAGGAGGAGATGCAT
SNV3_AL1	X	GAAGGTGACCAAGTTCATGCTTCACCACCATAGAACCACC
SNV3_AL2	Y	GAAGGTCGGAGTCAACGGATTGCTTCACCACCATAGAACCACT
SNV3_C	Common	GGGATGAGATGCCATTCTTCCAAATAATA
SNV4_AL1	Y	GAAGGTGACCAAGTTCATGCTCGCCCTCAGCCTGGTTGAT
SNV4_AL2	X	GAAGGTCGGAGTCAACGGATTGCGCCTCAGCCTGGTTGAG
SNV4_C	Common	TCGTCATGCACTCCTTCACAGCTTT
SNV5_AL1	X	GAAGGTGACCAAGTTCATGCTGGAATTTGCCTGAAATAATGAATGAATATG
SNV5_AL2	Y	GAAGGTCGGAGTCAACGGATTGTGGAATTTGCCTGAAATAATGAATGAATATA
SNV5_C	Common	AGGACATTACAGATTGGTCAGACCATATA
SNV6_AL1	X	GAAGGTGACCAAGTTCATGCTTACCCTTCTCACCACCTGTTT
SNV6_AL2	Y	GAAGGTCGGAGTCAACGGATTCTTACCCTTCTCACCACCTGTTG
SNV6_C	Common	CATAGTTCTTACCCTTACTGTACCAGATA
SNV7_AL1	Y	GAAGGTGACCAAGTTCATGCTCAGTGAACCTCCCTATGAGGCA
SNV7_AL2	X	GAAGGTCGGAGTCAACGGATTAGTGAACCTCCCTATGAGGCG
SNV7_C	Common	CTCGGTACAAGGTTGAAAGATGAAAGATA

Table 2: Genome assembly statistics for *P. fluviatilis* and *P. schrenkii*. For comparison, the table also provides numbers for two recently published *Perca sp.* assemblies [9,64]. Abbreviations: LR = long reads; HiC = chromosome conformation capture; CG = comparative genomics; 10X = linked-read sequencing; GLM = genetic linkage map.

	this study			earlier studies		
Species	<i>P. fluviatilis</i>	<i>P. schrenkii</i>	<i>S. vitreus</i>	<i>P. flavescens</i>	<i>P. fluviatilis</i>	<i>S. lucioperca</i>
Strategy	LR+HiC	LR+CG	LR+CG	LR+10X+HiC	10X	LR+GLM
total length	951,362,726	908,224,480	791,708,797	877,456,336	958,225,486	901,238,333
longest 24 sequences assembly fraction	99.0%	94.7%	96.5%	98.8%	41.4%	99.5%
scaffold/chromosome N50	39,550,354	36,400,992	33,333,317	37,412,490	6,260,519	41,060,379
contig N50	4,101,751	3,162,456	6,206,245	4,268,950	12,991	6,160,542

Table 3: BUSCO scoring of annotations of five Percidae genome assemblies (*P. fluviatilis*, *P. schrenkii*, *S. vitreus* from this study). The comparative mapping of high quality NCBI/GNOMON annotations onto closely related species' genome assemblies is a cost-effective and fast procedure to annotate new genomes. Abbreviations used: C = complete; S = single copy; D = duplicated; F = fragmented; M = missing.

	Species	Annotation type	BUSCO scoring code
# 1	<i>P. fluviatilis</i>	NCBI/GNOMON	C: 98.5% [S: 95.3%, D: 3.2%], F: 1.0%, M: 0.5%, n: 4584
# 2	<i>P. flavescens</i>	NCBI/GNOMON	C: 99.3% [S: 95.9%, D: 3.4%], F: 0.5%, M: 0.2%, n: 4584
# 3	<i>P. schrenkii</i>	mapping of annot. #2	C: 95.9% [S: 92.6%, D: 3.3%], F: 2.8%, M: 1.3%, n: 4584
# 4	<i>S. lucioperca</i>	NCBI/GNOMON	C: 99.3% [S: 95.9%, D: 3.4%], F: 0.5%, M: 0.2%, n: 4584
# 5	<i>S. vitreus</i>	mapping of annot. #4	C: 98.6% [S: 95.5%, D: 3.1%], F: 0.8%, M: 0.6%, n: 4584

Table 4: Sex-linkage of different sex-markers in *Perca fluviatilis* and *Perca schrenkii*. Associations between each sex-specific marker and sex phenotypes are provided for both males and females (number of positive individuals / total number of individuals) along with the p-value of association with sex that was calculated for each species and population based on the Pearson's Chi-square test with Yates' continuity correction. ns = not statistically significant.

Species	Population	marker	males	females	p value
<i>Perca schrenkii</i>	Alakol Lake, Kazakhstan	<i>amhr2bY</i>	1/1	0/1	ns
<i>Perca fluviatilis</i>	Mueggelsee Lake Germany	<i>hsdl1</i>	10/10	0/9	9.667e-05
<i>Perca fluviatilis</i>	Lucas Perche, France	SNV1	48/48	0/47	< 2.2e-16
<i>Perca fluviatilis</i>	Kortowskie Lake, Poland	SNV1	17/17	0/20	8.83e-09

Table 5: KASpar allele-specific PCR assays on seven single sex-specific nucleotide variations (SNV ID#) in *P. fluviatilis*. Numbers of homozygote (Ho), heterozygote (He) and uncalled genotypes (U). N = Total numbers of genotyped individuals (M/F: Males/females), %N = percentage of genotyped individuals, % As = percentage of correctly assigned genotypes i.e., male heterozygotes and female homozygotes. The p-value of association with sex was calculated for each SNV based on the Pearson's Chi-square test with Yates' continuity correction scoring heterozygote males and homozygote females as positives.

SNV ID#	N (M/F)	% N	M Ho/He/U	F Ho/He/U	% As	p value
SNV1	95 (48/47)	99,0	0/48/0	47/0/0	100,0	< 2.2e-16
SNV2	96 (48/48)	100,0	8/37/3	34/2/12	74,0	3.175e-11
SNV3	93 (45/48)	96,9	0/45/0	48/0/0	100,0	< 2.2e-16
SNV4	96 (48/48)	100,0	0/46/2	46/0/2	95,8	< 2.2e-16
SNV5	92 (44/48)	95,8	0/42/2	46/0/2	95,7	< 2.2e-16
SNV6	93 (48/45)	96,9	1/47/0	25/2/18	77,4	1.964e-14
SNV7	95 (47/48)	99,0	1/46/0	45/3/0	95,8	< 2.2e-16

676 **Supplementary Table 1:** Annotated repeats in *Perca sp.* and *Sander sp.* genomes (RepeatModeler *de*
677 *novi* analysis). Repeat elements mentioned in the manuscript have grey highlighting. The class “DNA”
678 is assigned to repeat elements that harbor signals of transposases, but miss further signals to classify
679 them with more detail.

	<i>P. fluviatilis</i>	<i>P. flavescens</i>	<i>P. schrenkii</i>	<i>S. lucioperca</i>	<i>S. vitreus</i>
length (no gaps)	951.053.269	877.041.836	893.440.234	901.028.039	785.350.625
Repeat class	bp masked	bp masked	bp masked	bp masked	bp masked
DNA	22.711.613	20.520.179	23.132.743	19.957.261	15.428.015
Academ	2.340.071	1.619.886	1.842.836	2.412.073	1.790.843
CMC-Chapaev-3	230.562	0	0	0	0
CMC-EnSpm	9.118.071	7.588.794	4.039.674	5.928.087	3.520.268
Crypton	841.031	547.307	748.707	772.498	402.911
Crypton-V	11.212	0	0	0	0
Dada	0	33.030	206.119	0	0
Ginger	0	15.288	0	0	0
IS3EU	1.282.033	531.773	496.067	288.665	509.614
Kolobok-Hydra	0	648.047	0	0	70.720
Kolobok-T2	1.252.506	1.976.511	2.668.034	1.586.132	1.222.046
MULE-MuDR	251.959	1.716.319	441.114	266.625	27.741
Maverick	2.187.699	1.402.756	266.487	1.342.717	0
Merlin	0	0	0	122.531	94.494
Novosib	0	0	0	0	82.199
P	467.516	442.149	411.688	765.209	555.234
PIF-Harbinger	12.989.790	12.205.497	12.181.221	12.830.055	8.037.073
PIF-ISL2EU	0	235.589	464.262	1.597.340	914.106
PiggyBac	3.844.887	2.011.288	2.742.549	3.776.961	2.299.194
Sola	1.885.532	229.560	163.435	77.871	0
TcMar	17.070	135.873	0	185.840	137.413
TcMar-Fot1	0	30.498	0	44.754	37.051
TcMar-ISRM11	4.570.634	3.171.866	2.722.899	2.158.133	1.830.923
TcMar-Stowaway	220.092	98.992	114.404	65.697	0
TcMar-Tc1	15.259.371	12.137.252	12.302.578	6.557.230	10.225.920
TcMar-Tc2	627.258	465.068	299.455	227.802	468.716
Zator	0	119.597	0	0	0
Zisupton	30.281	0	127.852	0	104.202

Zisupton-hAT-hybrid	0	0	0	0	339.346
hAT	9.251.059	7.244.672	9.113.922	8.460.295	6.356.798
hAT-Ac	26.161.464	27.815.352	29.153.525	30.578.355	27.361.032
hAT-Blackjack	1.252.051	459.611	338.327	514.383	437.930
hAT-Charlie	7.578.170	5.645.728	8.825.006	5.557.301	3.893.733
hAT-Tip100	3.892.297	2.083.169	5.060.148	2.183.415	2.136.454
hAT-Tol2	7.383.933	7.130.470	10.507.431	6.788.875	4.948.115
hAT-hAT5	1.008.628	1.141.196	1.066.203	873.439	560.575
hAT-hAT6	153.938	129.767	0	0	37.338
hAT-hobo	693.242	589.992	435.263	245.056	840.680
LINE	253.345	0	0	135.963	162.701
CR1	61.557	52.996	46.593	68.770	58.461
Dong-R4	0	161.938	0	0	0
I	902.480	1.009.950	1.721.862	451.473	448.921
I-Nimb	187.474	66.650	179.364	0	89.737
Jockey	1.281.097	0	0	249.376	0
L1	3.161.932	2.720.443	3.146.061	3.530.190	3.456.430
L1-Tx1	1.332.071	707.047	492.758	1.328.940	247.067
L2	24.295.832	18.778.236	18.931.729	15.671.956	10.981.470
Penelope	696.540	651.596	168.974	978.870	436.687
Proto2	432.031	406.555	335.607	288.595	210.869
R1	0	0	0	146.213	277.081
R2-Hero	258.797	37.021	152.400	101.778	204.860
R2-NeSL	139.492	0	191.055	106.574	62.871
RTE	1.012.896	0	0	0	0
RTE-BovB	3.915.100	11.058.368	4.053.280	5.607.772	8.522.404
RTE-RTE	0	0	0	169.573	0
RTE-RTEX	0	26.699	19.406	32.367	0
RTE-X	738.450	801.862	1.308.994	1.325.349	418.476
Rex-Babar	8.447.394	7.183.710	11.161.891	7.936.953	5.965.113
Tad1	0	0	0	138.056	320.275
LTR	569.316	146.042	61.769	0	0
Copia	180.685	275.175	422.246	471.447	0

DIRS	766.684	743.991	1.555.092	1.105.144	825.655
ERV1	750.875	1.123.315	980.225	1.469.763	126.774
ERVK	659.689	486.486	0	513.490	3.133.108
Gypsy	2.510.567	2.056.070	3.675.723	2.213.161	1.672.149
Ngaro	980.001	3.390.987	850.690	768.211	292.619
Pao	419.975	385.357	723.976	1.151.953	307.558
RC	0	0	0	0	0
Helitron	6.307.248	3.514.054	4.649.952	5.159.806	2.433.280
Retroposon	213.419	116.255	421.490	238.385	0
SINE	1.210.545	1.637.348	1.401.793	1.524.037	936.353
5S-Deu-L2	721.151	965.222	838.622	0	873.243
ID	0	0	19.012	29.728	116.970
MIR	1.185.268	1.020.008	1.163.355	2.103.257	382.739
tRNA	3.640.638	3.701.722	3.698.003	3.271.022	3.693.238
tRNA-Core	0	0	0	0	293.857
tRNA-Core-L2	0	0	0	89.805	106.872
tRNA-Deu-L2	0	0	0	42.616	0
tRNA-L2	461.844	0	103.308	223.271	301.117
tRNA-V	0	0	492.471	0	0
Unknown	149.784.304	121.893.498	134.020.433	144.621.637	113.225.894
total interspersed	354.992.667	305.241.677	326.860.083	319.430.101	255.255.533
Low_complexity	2.964.797	2.285.494	2.321.578	2.478.451	2.097.985
Satellite	700.110	1.425.777	1.023.206	656.699	1.718.620
Simple_repeat	30.391.090	32.172.324	29.527.186	34.124.020	27.469.062
rRNA	358.199	351.617	313.179	42.963	708.978
snRNA	0	0	0	9.265	0
Total	389.406.863	341.476.889	360.045.232	356.741.499	287.250.178

680

681

682 REFERENCES

- 683 1. Stepien CA, Haponski AE. Taxonomy, Distribution, and Evolution of the Percidae. In: Kestemont
684 P, Dabrowski K, Summerfelt RC, editors. *Biology and Culture of Percid Fishes: Principles and*
685 *Practices*. Dordrecht: Springer Netherlands;
- 686 2. Hermelink B, Wuertz S, Trubiroha A, Rennert B, Kloas W, Schulz C. Influence of temperature on
687 puberty and maturation of pikeperch, *Sander lucioperca*. *Gen Comp Endocrinol*. 2011; doi:
688 10.1016/j.ygcen.2011.03.013.
- 689 3. Schaefer FJ, Overton JL, Kloas W, Wuertz S. Length rather than year-round spawning, affects
690 reproductive performance of RAS-reared F-generation pikeperch, *Sander lucioperca* (Linnaeus, 1758)
691 - Insights from practice. *J Appl Ichthyol*. 2018; doi: 10.1111/jai.13628.
- 692 4. Policar T, Schaefer FJ, Panana E, Meyer S, Teerlinck S, Toner D, et al.. Recent progress in
693 European percid fish culture production technology-tackling bottlenecks (vol 27, pg 4, 2019).
694 *Aquacult Int*. 2019; doi: 10.1007/s10499-019-00457-4.
- 695 5. Malison JA, Kayes TB, Best CD, Amundson CH, Wentworth BC. Sexual Differentiation and Use of
696 Hormones to Control Sex in Yellow Perch (*Perca flavescens*). *Can J Fish Aquat Sci*. 1986; doi:
697 10.1139/f86-004.
- 698 6. Melard C, Kestemont P, Grignard JC. Intensive culture of juvenile and adult Eurasian perch (*P-*
699 *fluviatilis*): Effect of major biotic and abiotic factors on growth. *J Appl Ichthyol*. 1996; doi: DOI
700 10.1111/j.1439-0426.1996.tb00085.x.
- 701 7. Rougeot C, Jacobs B, Kestemont P, Melard C. Sex control and sex determinism study in Eurasian
702 perch, *Perca fluviatilis*, by use of hormonally sex-reversed male breeders. *Aquaculture*. 2002; doi: Pii
703 S0044-8486(01)00893-6 Doi 10.1016/S0044-8486(01)00893-6.
- 704 8. Rougeot C, Ngingo JV, Gillet L, Vanderplasschen A, Melard C. Gynogenesis induction and sex
705 determination in the Eurasian perch, *Perca fluviatilis*. *Aquaculture*. 2005; doi:
706 10.1016/j.aquaculture.2004.11.004.
- 707 9. Feron R, Zahm M, Cabau C, Klopp C, Roques C, Bouchez O, et al.. Characterization of a Y-
708 specific duplication/insertion of the anti-Müllerian hormone type II receptor gene based on a
709 chromosome-scale genome assembly of yellow perch, *Perca flavescens*. *Mol Ecol Resour*. 2020; doi:
710 10.1111/1755-0998.13133.
- 711 10. Pan Q, Kay T, Depincé A, Adolphi M, Scharl M, Guiguen Y, et al.. Evolution of master sex
712 determiners: TGF- β signalling pathways at regulatory crossroads. *Philos Trans R Soc Lond B Biol Sci*.
713 2021; doi: 10.1098/rstb.2020.0091.
- 714 11. Pan Q, Feron R, Jouanno E, Darras H, Herpin A, Koop B, et al.. The rise and fall of the ancient
715 northern pike master sex-determining gene. Przeworski M, Weigel D, editors. *eLife*. eLife Sciences
716 Publications, Ltd; 2021; doi: 10.7554/eLife.62858.
- 717 12. Pan Q, Feron R, Yano A, Guyomard R, Jouanno E, Vigouroux E, et al.. Identification of the
718 master sex determining gene in Northern pike (*Esox lucius*) reveals restricted sex chromosome
719 differentiation. *PLOS Genetics*. 2019; doi: 10.1371/journal.pgen.1008013.
- 720 13. Li M, Sun Y, Zhao J, Shi H, Zeng S, Ye K, et al.. A Tandem Duplicate of Anti-Müllerian

721 Hormone with a Missense SNP on the Y Chromosome Is Essential for Male Sex Determination in Nile
722 Tilapia, *Oreochromis niloticus*. *PLOS Genetics*. 2015; doi: 10.1371/journal.pgen.1005678.

723 14. Holborn MK, Einfeldt AL, Kess T, Duffy SJ, Messmer AM, Langille BL, et al.. Reference genome
724 of lumpfish *Cyclopterus lumpus* Linnaeus provides evidence of male heterogametic sex determination
725 through the AMH pathway. *Mol Ecol Resour*. 2022; doi: 10.1111/1755-0998.13565.

726 15. Song W, Xie Y, Sun M, Li X, Fitzpatrick CK, Vaux F, et al.. A duplicated amh is the master sex-
727 determining gene for *Sebastes rockfish* in the Northwest Pacific. *Open Biol*. 2021; doi:
728 10.1098/rsob.210063.

729 16. Rondeau EB, Laurie CV, Johnson SC, Koop BF. A PCR assay detects a male-specific duplicated
730 copy of Anti-Müllerian hormone (amh) in the lingcod (*Ophiodon elongatus*). *BMC Res Notes*. 2016;
731 doi: 10.1186/s13104-016-2030-6.

732 17. Hattori RS, Murai Y, Oura M, Masuda S, Majhi SK, Sakamoto T, et al.. A Y-linked anti-Müllerian
733 hormone duplication takes over a critical role in sex determination. *Proc Natl Acad Sci USA*. 2012;
734 doi: 10.1073/pnas.1018392109.

735 18. Wen M, Pan Q, Jouanno E, Montfort J, Zahm M, Cabau C, et al.. An ancient truncated duplication
736 of the anti-Müllerian hormone receptor type 2 gene is a potential conserved master sex determinant in
737 the Pangasiidae catfish family. *Mol Ecol Resour*. 2022; doi: 10.1111/1755-0998.13620.

738 19. Kamiya T, Kai W, Tasumi S, Oka A, Matsunaga T, Mizuno N, et al.. A trans-species missense
739 SNP in *Amhr2* is associated with sex determination in the tiger pufferfish, *Takifugu rubripes* (fugu).
740 *PLoS Genet*. 2012; doi: 10.1371/journal.pgen.1002798.

741 20. Nakamoto M, Uchino T, Koshimizu E, Kuchiishi Y, Sekiguchi R, Wang L, et al.. A Y-linked anti-
742 Müllerian hormone type-II receptor is the sex-determining gene in ayu, *Plecoglossus altivelis*. *PLoS*
743 *Genet*. 2021; doi: 10.1371/journal.pgen.1009705.

744 21. Qu M, Liu Y, Zhang Y, Wan S, Ravi V, Qin G, et al.. Seadragon genome analysis provides
745 insights into its phenotype and sex determination locus. *Sci Adv*. 2021; doi: 10.1126/sciadv.abg5196.

746 22. Nguinkal JA, Brunner RM, Verleih M, Rebl A, de los Rios-Perez L, Schafer N, et al.. The First
747 Highly Contiguous Genome Assembly of Pikeperch (*Sander lucioperca*), an Emerging Aquaculture
748 Species in Europe. *Genes-Basel*. 2019; doi: ARTN 708 10.3390/genes10090708.

749 23. Malmstrom M, Matschiner M, Torresen OK, Jakobsen KS, Jentoft S. Whole genome sequencing
750 data and de novo draft assemblies for 66 teleost species. *Sci Data*. 2017; doi: ARTN 160132
751 10.1038/sdata.2016.132.

752 24. Foissac S, Djebali S, Munyard K, Vialaneix N, Rau A, Muret K, et al.. Multi-species annotation of
753 transcriptome and chromatin structure in domesticated animals. *BMC Biology*. 2019; doi:
754 10.1186/s12915-019-0726-5.

755 25. Wick RR, Judd LM, Gorrie CL, Holt KE. Completing bacterial genome assemblies with multiplex
756 MinION sequencing. *Microb Genom*. 2017; doi: 10.1099/mgen.0.000132.

757 26. Hailin Liu SW. SMARTdenovo: a de novo assembler using long noisy reads. *Gigabyte*. 2021; doi:
758 10.46471/gigabyte.15.

759 27. Li H. Minimap2: pairwise alignment for nucleotide sequences. *Bioinformatics*. 2018; doi:

760 10.1093/bioinformatics/bty191.

761 28. Vaser R, Sović I, Nagarajan N, Šikić M. Fast and accurate de novo genome assembly from long
762 uncorrected reads. *Genome Res.* 2017; doi: 10.1101/gr.214270.116.

763 29. Li H. Aligning sequence reads, clone sequences and assembly contigs with BWA-MEM.
764 *arXiv:13033997 [q-bio]*. 2013;

765 30. Walker BJ, Abeel T, Shea T, Priest M, Abouelliel A, Sakthikumar S, et al.. Pilon: an integrated
766 tool for comprehensive microbial variant detection and genome assembly improvement. *PLoS ONE*.
767 2014; doi: 10.1371/journal.pone.0112963.

768 31. Durand NC, Shamim MS, Machol I, Rao SSP, Huntley MH, Lander ES, et al.. Juicer Provides a
769 One-Click System for Analyzing Loop-Resolution Hi-C Experiments. *Cell Syst.* 2016; doi:
770 10.1016/j.cels.2016.07.002.

771 32. Dudchenko O, Batra SS, Omer AD, Nyquist SK, Hoeger M, Durand NC, et al.. De novo assembly
772 of the *Aedes aegypti* genome using Hi-C yields chromosome-length scaffolds. *Science*. 2017; doi:
773 10.1126/science.aal3327.

774 33. Robinson JT, Turner D, Durand NC, Thorvaldsdottir H, Mesirov JP, Aiden EL. Juicebox.js
775 Provides a Cloud-Based Visualization System for Hi-C Data. *Cell Syst.* 2018; doi:
776 10.1016/j.cels.2018.01.001.

777 34. Xu GC, Xu TJ, Zhu R, Zhang Y, Li SQ, Wang HW, et al.. LR_Gapcloser: a tiling path-based gap
778 closer that uses long reads to complete genome assembly. *Gigascience*. 2019; doi: ARTN giy157
779 10.1093/gigascience/giy157.

780 35. Garrison E MG. Haplotype-based variant detection from short-read sequencing. *arXiv preprint*
781 *arXiv:12073907 [q-bioGN]*. 2012;

782 36. Bolger AM, Lohse M, Usadel B. Trimmomatic: a flexible trimmer for Illumina sequence data.
783 *Bioinformatics*. 2014; doi: 10.1093/bioinformatics/btu170.

784 37. Peng Y, Leung HC, Yiu SM, Chin FY. IDBA-UD: a de novo assembler for single-cell and
785 metagenomic sequencing data with highly uneven depth. *Bioinformatics*. 2012; doi:
786 10.1093/bioinformatics/bts174.

787 38. Kuhl H, Li L, Wuertz S, Stock M, Liang XF, Klopp C. CSA: A high-throughput chromosome-
788 scale assembly pipeline for vertebrate genomes. *Gigascience*. 2020; doi: 10.1093/gigascience/giaa034.

789 39. Kolmogorov M, Yuan J, Lin Y, Pevzner PA. Assembly of long, error-prone reads using repeat
790 graphs. *Nat Biotechnol.* 2019; doi: 10.1038/s41587-019-0072-8.

791 40. Iwata H, Gotoh O. Benchmarking spliced alignment programs including Spaln2, an extended
792 version of Spaln that incorporates additional species-specific features. *Nucleic Acids Res.* 2012; doi:
793 ARTN e161 10.1093/nar/gks708.

794 41. Simao FA, Waterhouse RM, Ioannidis P, Kriventseva EV, Zdobnov EM. BUSCO: assessing
795 genome assembly and annotation completeness with single-copy orthologs. *Bioinformatics*. 2015; doi:
796 10.1093/bioinformatics/btv351.

797 42. Kuhn RM, Haussler D, Kent WJ. The UCSC genome browser and associated tools. *Brief*

798 *Bioinform.* 2013; doi: 10.1093/bib/bbs038.

799 43. Kent WJ. BLAT - The BLAST-like alignment tool. *Genome Res.* 2002; doi: 10.1101/gr.229202.

800 44. He S, Li L, Lv LY, Cai WJ, Dou YQ, Li J, et al.. Mandarin fish (Sinipercaidae) genomes provide
801 insights into innate predatory feeding. *Commun Biol.* 2020; doi: ARTN 361 10.1038/s42003-020-
802 1094-y.

803 45. Frith MC, Kawaguchi R. Split-alignment of genomes finds orthologies more accurately. *Genome*
804 *Biol.* 2015; doi: ARTN 106 10.1186/s13059-015-0670-9.

805 46. Blanchette M, Kent WJ, Riemer C, Elnitski L, Smit AF, Roskin KM, et al.. Aligning multiple
806 genomic sequences with the threaded blockset aligner. *Genome Res.* 2004; doi: 10.1101/gr.1933104.

807 47. Kozlov AM, Darriba D, Flouri T, Morel B, Stamatakis A. RAxML-NG: a fast, scalable and user-
808 friendly tool for maximum likelihood phylogenetic inference. *Bioinformatics.* 2019; doi:
809 10.1093/bioinformatics/btz305.

810 48. Minh BQ, Schmidt HA, Chernomor O, Schrempf D, Woodhams MD, von Haeseler A, et al.. IQ-
811 TREE 2: New Models and Efficient Methods for Phylogenetic Inference in the Genomic Era. *Mol Biol*
812 *Evol.* 2020; doi: 10.1093/molbev/msaa015.

813 49. Yang Z. PAML 4: phylogenetic analysis by maximum likelihood. *Mol Biol Evol.* 2007; doi:
814 10.1093/molbev/msm088.

815 50. Amores A, Catchen J, Ferrara A, Fontenot Q, Postlethwait JH. Genome evolution and meiotic
816 maps by massively parallel DNA sequencing: spotted gar, an outgroup for the teleost genome
817 duplication. *Genetics.* 2011; doi: 10.1534/genetics.111.127324.

818 51. Catchen JM, Amores A, Hohenlohe P, Cresko W, Postlethwait JH. Stacks: building and
819 genotyping Loci de novo from short-read sequences. *G3 (Bethesda).* 2011; doi:
820 10.1534/g3.111.000240.

821 52. Feron R, Pan Q, Wen M, Imarazene B, Jouanno E, Anderson J, et al.. RADSex: A computational
822 workflow to study sex determination using restriction site-associated DNA sequencing data. *Mol Ecol*
823 *Resour.* 2021; doi: 10.1111/1755-0998.13360.

824 53. Imarazene B, Du K, Beille S, Jouanno E, Feron R, Pan Q, et al.. A supernumerary “B-sex”
825 chromosome drives male sex determination in the Pachón cavefish, *Astyanax mexicanus*. *Curr Biol.*
826 2021; doi: 10.1016/j.cub.2021.08.030.

827 54. Wen M, Pan Q, Larson W, Ech  C, Guiguen Y. Characterization of the sex determining region of
828 channel catfish (*Ictalurus punctatus*) and development of a sex-genotyping test. *Gene.* 2023; doi:
829 10.1016/j.gene.2022.146933.

830 55. Jasonowicz AJ, Simeon A, Zahm M, Cabau C, Klopp C, Roques C, et al.. Generation of a
831 chromosome-level genome assembly for Pacific halibut (*Hippoglossus stenolepis*) and
832 characterization of its sex-determining genomic region. *Mol Ecol Resour.* 2022; doi: 10.1111/1755-
833 0998.13641.

834 56. Smith SM, Maughan PJ. SNP genotyping using KASPar assays. *Methods Mol Biol.* 2015; doi:
835 10.1007/978-1-4939-1966-6_18.

836 57. Pasquier J, Cabau C, Nguyen T, Jouanno E, Severac D, Braasch I, et al.. Gene evolution and gene
837 expression after whole genome duplication in fish: the PhyloFish database. *BMC Genomics*. 2016; doi:
838 10.1186/s12864-016-2709-z.

839 58. Kim D, Langmead B, Salzberg SL. HISAT: a fast spliced aligner with low memory requirements.
840 *Nat Methods*. 2015; doi: 10.1038/nmeth.3317.

841 59. Pertea M, Pertea GM, Antonescu CM, Chang T-C, Mendell JT, Salzberg SL. StringTie enables
842 improved reconstruction of a transcriptome from RNA-seq reads. *Nat Biotechnol*. 2015; doi:
843 10.1038/nbt.3122.

844 60. Braun EL, Kimball RT. Data Types and the Phylogeny of Neoaves. *Birds*. 2:1–222021;

845 61. Jarvis ED, Mirarab S, Aberer AJ, Li B, Houde P, Li C, et al.. Whole-genome analyses resolve
846 early branches in the tree of life of modern birds. *Science*. 2014; doi: 10.1126/science.1253451.

847 62. Kuhl H, Frankl-Vilches C, Bakker A, Mayr G, Nikolaus G, Boerno ST, et al.. An Unbiased
848 Molecular Approach Using 3'-UTRs Resolves the Avian Family-Level Tree of Life. *Mol Biol Evol*.
849 2021; doi: 10.1093/molbev/msaa191.

850 63. Heldin C-H, Moustakas A. Signaling Receptors for TGF- β Family Members. *Cold Spring Harb*
851 *Perspect Biol*. 2016; doi: 10.1101/cshperspect.a022053.

852 64. Ozerov MY, Ahmad F, Gross R, Pukk L, Kahar S, Kisand V, et al.. Highly Continuous Genome
853 Assembly of Eurasian Perch (*Perca fluviatilis*) Using Linked-Read Sequencing. *G3: Genes, Genomes,*
854 *Genetics*. 2018; doi: 10.1534/g3.118.200768.

855 65. Berv JS, Field DJ. Genomic Signature of an Avian Lilliput Effect across the K-Pg Extinction. *Syst*
856 *Biol*. 2018; doi: 10.1093/sysbio/syx064.

857 66. Cortez D, Marin R, Toledo-Flores D, Froidevaux L, Liechti A, Waters PD, et al.. Origins and
858 functional evolution of Y chromosomes across mammals. *Nature*. Nature Publishing Group; 2014;
859 doi: 10.1038/nature13151.

860 67. Pinto BJ, Gamble T, Smith CH, Wilson MA. A lizard is never late: squamate genomics as a recent
861 catalyst for understanding sex chromosome and microchromosome evolution. bioRxiv;

862 68. Yano A, Nicol B, Jouanno E, Quillet E, Fostier A, Guyomard R, et al.. The sexually dimorphic on
863 the Y-chromosome gene (sdY) is a conserved male-specific Y-chromosome sequence in many
864 salmonids. *Evol Appl*. 2013; doi: 10.1111/eva.12032.

865 69. Bertho S, Herpin A, Scharl M, Guiguen Y. Lessons from an unusual vertebrate sex-determining
866 gene. *Philos Trans R Soc Lond B Biol Sci*. 2021; doi: 10.1098/rstb.2020.0092.

867 70. Hart KN, Stocker WA, Nagykerly NG, Walton KL, Harrison CA, Donahoe PK, et al.. Structure of
868 AMH bound to AMHR2 provides insight into a unique signaling pair in the TGF- β family. *Proc Natl*
869 *Acad Sci U S A*. 2021; doi: 10.1073/pnas.2104809118.

870 71. Meier M, Tokarz J, Haller F, Mindnich R, Adamski J. Human and zebrafish hydroxysteroid
871 dehydrogenase like 1 (HSDL1) proteins are inactive enzymes but conserved among species. *Chemico-*
872 *biological interactions*. Chem Biol Interact; 2009; doi: 10.1016/j.cbi.2008.10.036.

873 72. Xiao L, Guo Y, Wang D, Zhao M, Hou X, Li S, et al.. Beta-Hydroxysteroid Dehydrogenase Genes

874 in Orange-Spotted Grouper (*Epinephelus coioides*): Genome-Wide Identification and Expression
875 Analysis During Sex Reversal. *Front Genet.* 2020; doi: 10.3389/fgene.2020.00161.

876 73. Fan B, Xie D, Li Y, Wang X, Qi X, Li S, et al.. A single intronic single nucleotide polymorphism
877 in splicing site of steroidogenic enzyme hsd17b1 is associated with phenotypic sex in oyster pompano,
878 *Trachinotus anak*. *Proc Biol Sci.* 2021; doi: 10.1098/rspb.2021.2245.

879 74. Koyama T, Nakamoto M, Morishima K, Yamashita R, Yamashita T, Sasaki K, et al.. A SNP in a
880 Steroidogenic Enzyme Is Associated with Phenotypic Sex in *Seriola* Fishes. *Current Biology.* 2019;
881 doi: 10.1016/j.cub.2019.04.069.

882 75. Purcell CM, Seetharam AS, Snodgrass O, Ortega-García S, Hyde JR, Severin AJ. Insights into
883 teleost sex determination from the *Seriola dorsalis* genome assembly. *BMC Genomics.* 2018; doi:
884 10.1186/s12864-017-4403-1.

885 76. Ko HW, Norman RX, Tran J, Fuller KP, Fukuda M, Eggenschwiler JT. Broad-Minded Links Cell
886 Cycle-Related Kinase to Cilia Assembly and Hedgehog Signal Transduction. *Developmental Cell.*
887 2010; doi: 10.1016/j.devcel.2009.12.014.

888 77. HUANG C-CJ, YAO HH-C. Diverse Functions of Hedgehog Signaling in Formation and
889 Physiology of Steroidogenic Organs. *Mol Reprod Dev.* 2010; doi: 10.1002/mrd.21174.

890 78. Guiguen Y, Fostier A, Piferrer F, Chang C-F. Ovarian aromatase and estrogens: a pivotal role for
891 gonadal sex differentiation and sex change in fish. *Gen Comp Endocrinol.* 2010; doi:
892 10.1016/j.ygcen.2009.03.002.

893 79. Baroiller JF, Guiguen Y. Endocrine and environmental aspects of sex differentiation in
894 gonochoristic fish. *EXS.* :177–201 2001;

895